ABSTRACT

In this Thesis, a new designed biomaterial made out of short repetitive amphiphilic peptide sequence AcN-RADARADARADARADA-$CONH_2$ (RAD16-I) that self-assembles forming nanofiber networks (hydrogel scaffold) has been used as synthetic extracellular matrix analog for cell maintenance, proliferation and differentiation. This peptide has been functionalized with biological active motifs from extracellular matrix proteins including laminin-1 and collagen IV. The prototypic self-assembling peptide scaffold RAD16-I and its biologically active derivatives have been characterized and tested using several cellular systems such as human aortic endothelial cells (HAEC), mature hepatocytes and a putative liver progenitor cell line, Lig-8. The proteolysis of the peptide RAD16-I has been evaluated using trypsin as a proteolytic enzyme and the resulting fragments have been analyzed by MALDI-TOF and AFM. Moreover the second generation of RAD16-I-based biomaterials have been tested using HAEC and mature hepatocytes. With these systems we have shown that the development of a biomimetic matrix enhances as well as maintain tissue-specific functions. In particular, the results obtained in cell differentiation, proliferation and maintenance of cell function using the synthetic self-assembling peptide matrices, are comparable with the results obtained using natural biological matrices counterparts (Collagen-I and Matrigel). This indicates that our extracellular matrix analogs can replace the use of naturally-derived materials and suggests the use of these smart biomaterials with instructive capacity for cells in therapeutics. Moreover, the use of the self-assembling peptide RAD16-I in the recreation of a stem-cell niche proved to be highly efficient. We were able to control stem-cell kinetics (from symmetric to assymetric) inducing functional differentiation while maintaining a small proportion of undifferentiated cells. This striking results clearly indicate that we were able to obtain a stem-cell niche where primitive cells (Lig-8) undergo differentiation acquiring mature hepatic functions. We have developed a biomaterial platform that can be used for functionalization with innumerable biomolecules, with capacity to induce biological processes like differentiation, control of proliferation, metabolic function, etc. These biomaterials will have a strong impact in therapeutics and regenerative biology.

SUMARIO

En esta Tesis, un nuevo biomaterial de diseño compuesto por secuencias peptídicas repetitivas y amfifílicas que por autoensamblaje forma redes de nanofibras (e hidrogeles), AcN-RADARADARADARADA-$CONH_2$ (RAD16-I), se ha utilizado como análogo de la matriz extracelular para el mantenimiento, proliferación y diferenciación celular. Este péptido se ha funcionalizado con motivos biológicamente activos procedentes de proteínas de la matriz extracelular incluyendo laminina-1 y colágeno IV. El scaffold peptídico autoensamblante RAD16-I y sus derivados biológicamente activos se han caracterizado y probado utilizando diferentes sistemas celulares como puede ser células endoteliales de aorta humanas (HAEC), hepatocitos maduros y la línea progenitora de hígado Lig-8. La proteólisis de este péptido se ha evaluado utilizando tripsina como enzima proteolítico, y los fragmentos resultantes se han analizado por MALDI-TOF y AFM. Asimismo, la segunda generación de biomateriales basados en el RAD16-I se ha probado tanto con HAEC como hepatocitos maduros. Con estos sistemas hemos demostrado que el desarrollo de una matriz biomimética refuerza a la vez que mantiene las funciones específicas de cada tejido. En particular, los resultados obtenidos en diferenciación, proliferación y mantenimiento de la función celular utilizando los péptidos sintéticos auto-ensamblantes son comparables con los resultados que se obtienen usando matrices biológicas (Colágeno I y Matrigel). Esto indica que nuestros análogos de la matriz extracelular pueden reemplazar a los materiales naturales, y sugiere el uso de estos materiales inteligentes con capacidad instructiva en aplicaciones terapéuticas. Asimismo, se ha probado que el uso de estos péptidos auto-ensamblantes es eficiente en la construcción de un nicho de células madre. Hemos sido capaces de controlar la cinética celular (de simétrica a asimétrica) induciendo diferenciación funcional, a la vez que se mantenía una pequeña proporción de células no diferenciadas. Estos resultados indican claramente que hemos sido capaces de obtener un nicho donde células primitivas (Lig-8) se diferencian adquiriendo funciones de hepatocitos maduros. Hemos desarrollado una plataforma de biomateriales que se podrían utilizar para la funcionalización con innumerables biomoléculas con capacidad de inducir procesos biológicos como la diferenciación, proliferación y función metabólica. Estos biomateriales preveemos que tendrán un gran impacto en el área terapéutica y biología regenerativa.

SUMARI

En aquesta Tesi, un nou biomaterial de disseny composat per seqüències peptídiques repetitives i amfifíliques, que per autoensamblatge forma xarxes de nanofibres (i hidrogels), AcN-RADARADARADARADA-$CONH_2$, s´ha utilitzat com a anàleg de la matriu extracel·lular per al manteniment, proliferació i diferenciació cel·lular. Aquest pèptid s'ha funcionatitzat amb motius biològicament actius procedents de proteïnes de la matriz extracel·lular incloent laminina-1 i colàgen IV. El scaffold peptídic autoensamblant RAD16-I i els seus derivats biològicament actius s´han caracteritzat i provat utilitzant diferents sistemes cel·lulars com pot ser les cèl·lules d'aorta humanes (HAEC), hepatocits madurs i la línea progenitora de fetge (Lig-8). La proteòlisi d'aquest pèptid s'ha avaluat utilitzant tripsina com a enzim proteolític, i els fragments resultants s'han analitzat per MALDI-TOF i AFM. Així mateix, la segona generació de biomaterials basats en el RAD16-I s'ha provat tant amb HAEC com amb hepatocits madurs. Amb aquests sistemes hem demostrat que el desenvolupament d'una matriu biomiètica reforça, a la vegada que manté, les funcions específiques de cada teixit. En particular, els resultats obtinguts en diferenciació, proliferació i manteniment de la funció cel·lular utilitzant pèptids sintètics autoensamblants són comparables amb els resultats que s'obtenen utilitzant matrius biològiques (Colàgen I i Matrigel). Això indica que els nostres anàlegs de la matriu extracel·lular poden substituir als materials naturals, i suggereix l'ús d'aquests materials intel·ligents amb capacitat instructiva en aplicacions terapèutiques. Així mateix s'ha provat que l'ús d'aquests pèptids auto-ensamblants és eficient en la construcció d'un nínxol de cèl·lules mare. Hem sigut capaços de controlar la cinètica cel·lular (de simètrica a assimètrica) induint diferenciació funcional, a la vegada que es mantenia una petita proporció de cèl·lules no diferenciades. Aquests resultats indiquen clarament que hem sigue capaços d'obtenir un nínxol on cèl·lules primitives (Lig-8) es diferencien adquirint funcions d'hepatocits madurs. Hem desenvolupat una plataforma de biomaterials que es podrien utilitzar per la funcionalització amb innumerables biomolècules amb capacitat d'induir processos biològics com la diferenciació, proliferació i funció metabòlica. Aquests biomaterials, preveiem que tindran un gran impacte a l'àrea terapèutica i biología regenerativa.

INDEX

LIST OF TABLES

LIST OF FIGURES

LIST OF ABBREVIATIONS

ACC: acetyl-CoA carboxylase
AFM: Atomic force microscopy
BM: Basement membrane
BrdU: 5-bromo-2'-deoxyuridine
BSA: Bovine serum albumin
CD: Circular dichroism
DMSO: Dimethylsulfoxide
DNA: Deoxyribonucleic acid
EC: Endothelial cell
ECM: Extracellular matrix
EGF: Epidermal growth factor
ELISA: Enzyme linked immunosorbent assay
ESC: Embryonic stem cell
FD: Fluorescein diacetate
FDA: Food and Drug Administration
FGF: Fibroblast growth factor
HAEC: Human aortic endothelial cell
HCM: Hepatocyte culture medium
HGF: Hepatocyte growth factor
HNF4-α: Hepatocyte nuclear factor 4-α
HSC: Hematopoietic stem cells
HUVEC: Human umbilical vein endothelial cell
LDL: Low density lipoprotein
LIF: Leukaemia inhibitory factor
MALDI-TOF: Matrix assisted laser desorption ionization time of flight
MCC: 3-methyl-crotonyl-CoA carboxylase
MDR2: Multidrug resistant protein 2
MEF: Mouse embryonic fibroblasts
MMP: Matrix metalloproteases
NO: Nitric oxide
NPC: Non parenchymal cells
PBS: Phosphate buffered saline
PC: Pyruvate carboxylase
PCL: Poly(caprolactone)
PCR: Polymerase chain reaction

PDMS: Polydimethylsiloxane

PGA: Poly(glycolic) acid

PGLA: Poly(glycolic-lactic) acid

PHx: Partial hepatectomy

PLA: Poly(lactic) acid

PPC: Propionyl-CoA carboxylase

PPF: Poly(propylenfumarate)

RNA: Ribonucleic acid

RT-PCR: Reverse transcriptase polymerase chain reaction

SACK: Supression of assymetric cell kinetics

SEC: Sinusoidal endothelial cell

TAT: Tyrosine aminotransferase

Xs: Xanthosine

GLOSSARY

apical: describes the tip of a cell, a structure or an organ. The apical surface of an epithelial cell is the exposed free surface, opposite to the basal surface. The basal surface rests on the basal lamina that separates the epithelium from other tissue

basal: situated near the base. The basal surface of a cell is opposite to the apical surface.

basement membrane: thin mat of extracellular matrix that separates epithelial sheets, and many other types of cells such as muscle or fat cells, from connective tissue.

beta-sheet: common structural motif in proteins in which different sections of the polypeptide chain run alongside each other, joined together by hydrogen bonding between atoms of the polypeptide backbone.

blastomere: one of the cells formed by the cleavage of a fertilized egg.

catabolism: general term for the enzyme-catalyzed reactions in a cell by which complex molecules are degraded to simpler ones with the release of energy. Intermediates in these reactions are sometimes called catabolites.

cell cycle: reproductive cycle of a cell: the orderly sequence of events by which a cell duplicates its contents and divides into two.

cell division: separation of a cell into two daughter cells. In eukaryotic cells it entails division of the nucleus (mitosis) closely followed by division of the cytoplasm.

cell fate: in developmental biology, describes what a particlar cell at a given stage of development will normally give rise to.

cell line: population of cells of plant or animal origin capable of dividing indefinitely in culture.

denaturation: dramatic change in conformation of a protein or nucleic acid caused by heating or by exposure to chemicals and usually resulting in the loss of biological function.

differentiation: process by which a cell undergoes a change to an overtly specialized cell type.

DNA microarray: technique for analysing the simultaneous expression of large numbers of genes in cells, in which isolated cellular RNA is hybridized to a large array of short DNA probes immobilized on glass slides.

ectoderm: embryonic tissue that is the precursor of the epidermis and nervous system.

embryonic stem cell: cell derived from the inner cell mass of the early mammalian embryo that can give rise to all the cells in the body. It can be grown in culture, genetically modified and inserted into a blastocyst to develop a transgenic animal.

endoderm: embryonic tissue that is the precursor of the gut and associated organs.

endothelial cell: flattened cell type that forms a sheet (the endothelium) lining all blood vessels.

epithelium: coherent cell sheet formed from one or more layers of cells covering an external surface or lining a cavity.

extracellular matrix: complex network of polysaccharides (such as glycosaminoglycans or cellulose) and proteins (such as collagen) secreted by cells. Serves as a structural element in tissues and also influences their development and physiology.

genomics: the science of studying the DNA sequences and properties of entire genomes.

glycosaminoglycan: long, linear, highly charged polysaccharide composed of a repeating pair of sugars, one of which is always an amino sugar. Mainly found covalently linked to a protein core in extracellular matrix proteoglycans. Examples include chondroitin sulfate, hyaluronic acid and heparin.

growth factor: extracellular polypeptide signal molecule that can stimulate a cell to grow or proliferate. Examples are epidermal growth factor (EGF) or hepatocyte growth factor (HGF). Most growth factors also have other actions.

housekeeping gene: gene serving a function required in all the cell types of an organism, regardless of their specialized role.

mesoderm: embryonic tissue that is the precursor to muscle, connective tissue, skeleton and many of the internal organs.

metabolism: the sum of total of the chemical processes that take place in living cells.

mitogen: an extracellular substance, such as a growth factor, that stimulates cell proliferation.

p53: tumor suppressor gene found mutated in about half of human cancers. It encodes a gene regulatory protein that is activated by damage to DNA and is involved in blocking further progression through the cell cycle.

PCR (polymerase chain reaction): technique for amplifying specific regions of DNA by the use of sequence-specific primers and multiple cycles of DNA synthesis, each cycle being followed by a brief heat treatment to separate complementary strands.

protease: an enzyme, such as trypsin that degrades proteins by hydrolyzation of some of their peptide bonds.

stem cell: relatively undifferentiated cell that can continue dividing indefinetely, throwing off daughter cells that can undergo terminal differentiation into particular cell types.

transcription factor: term loosely applied to any protein required to initiate or regulate transcription in eucaryotes. Includes both gene regulatory proteins as well as the general transcription factors.

Chapter 1: *Introduction*

1.1. INTRODUCTION

1.1.1. Biomedical engineering and tissue engineering

Biomedical engineering is a discipline that integrates engineering and life sciences to improve human health. It is by nature a multidisciplinary science and it covers multiple application fields, some of which are shown in Figure 1.1. Many of these fields are often interconnected.

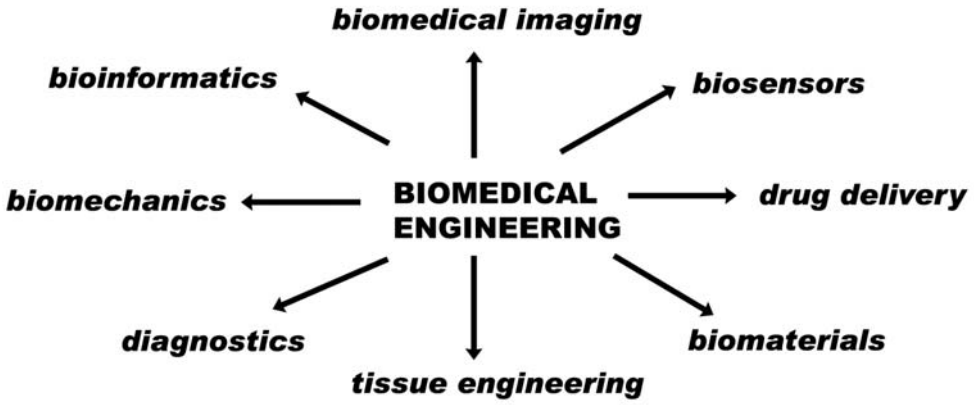

Figure 1.1. Scheme of biomedical technologies applications.

Tissue engineering is an emerging biomedical technology addressed to the treatment of patients needed of tissues or organs. This interdisciplinary field of research involves different scientific approaches including cell biology, materials science, and bioengineering towards the development of biological substitutes that will restore normal cell function (Godbey and Atala, 2002). Tissue engineering has an enormous potential for reparative medicine, as this discipline uses materials and technology to restore or improve function of organs and tissues affected by disease, injury or deformation (Sipe, 2002). Another application, not less interesting than that of the use of engineered tissues for implantation in regenerative medicine but probably less studied, is the use of these engineered tissue constructs for the study of physiology or pathophysiology *in vitro*. A functional *in vitro* tissue would be really useful to study the effects of drugs in that tissue (accelerating in this way the process of the application of new drugs), or the development of new therapies to treat some diseases (Griffith and Naughton, 2002; Griffith and Swartz, 2006).

The underlying concept for tissue engineering is the belief that cells can be isolated, expanded *in vitro* and seeded onto a carrier or scaffold prior to implantation.

This scaffold usually needs to be a highly porous artificial extracellular matrix analog, capable to accommodate mammalian cells and guide their growth and tissue regeneration in three dimensions (Yang *et al*., 2002). Isolated cells cannot always build a new tissue by themselves. Most of the time, the surrounding microenvironment, which is also instructive, is crucial for tissue growth and function. The cellular microenvironment is basically comprised of: signaling molecules such as growth factors or hormones, the extracellular matrix (ECM) molecules, physical or mechanical factors, and the presence of other types of cells interacting with them by cell-cell contacts. Therefore, the discovery and use of biomaterials capable to modulate cellular responses is a critical and limiting step in tissue engineering.

1.1.2. Biomaterials

Biomaterials are those materials intended to interface with biological systems, either to replace, reconstruct, enhance or support either tissues or tissue function.

Biomaterials have typically been metalic, ceramic and polymeric. Metalic materials are beeing used for long for prostheses; ceramics, specially hydroxyapatite has been used for bone reconstruction, and polymeric materials have been found to present innumberable applications, from surgical sutures and surgical glues to contact lenses, heart valves, etc...

For tissue engineering and regenerative medicine applications, a highly porous biomaterial or scaffold is usually needed to guide and accommodate the cells while promoting their function. The ideal scaffold for supporting cell attachment and growth should meet several criteria (Holmes *et al*., 2000):

- present building blocks derived from biomolecules
- have basic units that are amenable to design and modification to achieve specific needs
- present controlled rate of biodegradation and no cytotoxicity
- promote cell-substrate interactions
- elicit no immune responses and inflammation
- be easy to produce, purify and process
- be readily transportable
- present chemical compatibility with aqueous solutions and physiological conditions, and
- be able to integrate with other materials.

Many different polymeric biomaterials are being used for tissue engineering, and they can be classified as naturally derived materials and synthetic polymers (Godbey and Atala, 2002; Yang *et al*., 2002; Lanza *et al*., 2000).

Natural polymers such as collagens, hyaluronic acid, alginate and chitosan have been used as scaffolds to study the repair of nerves, skin, cartilage and bone (Pachence, 1996; Parenteau, ; Lee and Mooney, 2001; Flanagan, 2003).

Collagen is one of the most abundant protein in mammals, it is normally obtained and purified from animal and human tissues by an enzymatic treatment and salt/acid extraction. It is one of the most applied scaffolds for tissue engineering and it is used *in vitro* for the culture of many different types of cells. It also presents the advantage that is proteolitically degraded by cell-secreted proteases. The use of collagen has been approved by the United States Food and Drug Administration (FDA) for different medical applications such as the treatment of skin ulcers (Parenteau,), which is the case of Apligraf, approved in year 2000. Another collagen-based product InFuse Bone Graft, is indicated for the treatment of degenerative disc disease or for the healing of bone fractures.

Hyaluronic acid is a glycosaminoglycan found in nearly every mammalian tissue and fluid. This material has been can be chemically cross-linked or combined with other materials in order to obtain the desired mechanical properties. It is degraded by cellular hyaluronidase, and it has been used in many different applications (Drury and Mooney, 2003). Hyaluronic acid has been approved by the FDA in cosmetics as wrinkle fillers (Restylan), or for the treatment of osteoarthritis (Nuflexxa).

Alginate, is a polysaccharide obtained primarily form seaweed that has been used in a variety of medical applications including cell encapsulation and drug stabilization for delivery applications (Drury and Mooney, 2003). It can be chemically crosslinked to improve the mechanical properties, and it degradation occurs by hydrolysis. It has been approved by the FDA for the treatment of ulcers and severe burns (Phytacare), or in combination with collagen indicated for wound healing (Fibracol).

Chitosan is a naturally ocurring polysaccharide which has a similar structure to glycosaminoglycans. It is extracted from arthropod exoskeletons, and can be gelled in a wide array of conditions. It is enzymatically degradable by lysozyme and it has been used and modified to culture hepatocytes, neural tissue and bone (Lee and Mooney, 2001; Drury and Mooney, 2003).

Additionally, many different biomaterials have been tested in *in vitro* and clinical studies with more or less success, and they are under continuous research to launch new products and devices into the market and therapies into the clinic. Although they have clear advantages versus synthetic polymers because they simulate the natural cell microenvironment, they may suffer variations from batch to batch. In addition, the main limitation for their application is that they are isolated from biological tissues and may carry pathogens.

In the framework of biodegradable *synthetic polymers* the most broadly investigated are poly(glycolic acid) (PGA), poly(lactic acid) (PLA) and their copolymers (PGLA), (Figure 1.2. and Figure 1.3.). These materials provide rigid structures of medium mechanical strength with 50-100 μm pore size and 10-30 μm fiber diameter (Figure 1.3.), in which cells adhere and grow on a *pseudo* three-dimensional environment (Semino, 2003). As it can be seen in Figure 1.3., liver-derived progenitor cells adhere on the surface of the polymer forming a two-dimensional monolayer. These polymers have been approved by the FDA for several applications. Traditionally, the first FDA approved PLGA products were surgical sutures, but nowadays cover many other aplications. In the field of drug delivery, there are currently in the market several PLGA formulations. For example Abbot Laboratories have in the market Lucrin and Procrin, which are leuprolide acetate-loaded microspheres for the treatment of prostate cancer. As well, Novartis markets Sandostatin LAR, which are octreotide-loaded PLGA microspheres for the treatment of acromegalgy and grastric cancers. In addition, a cell-based PLGA device, Dermagraft, was approved by the FDA in 2001 for the treatment of skin ulcers. This dermal substitute is composed on human fibroblasts seeded in a PLGA mesh, which have secreted their own ECM.

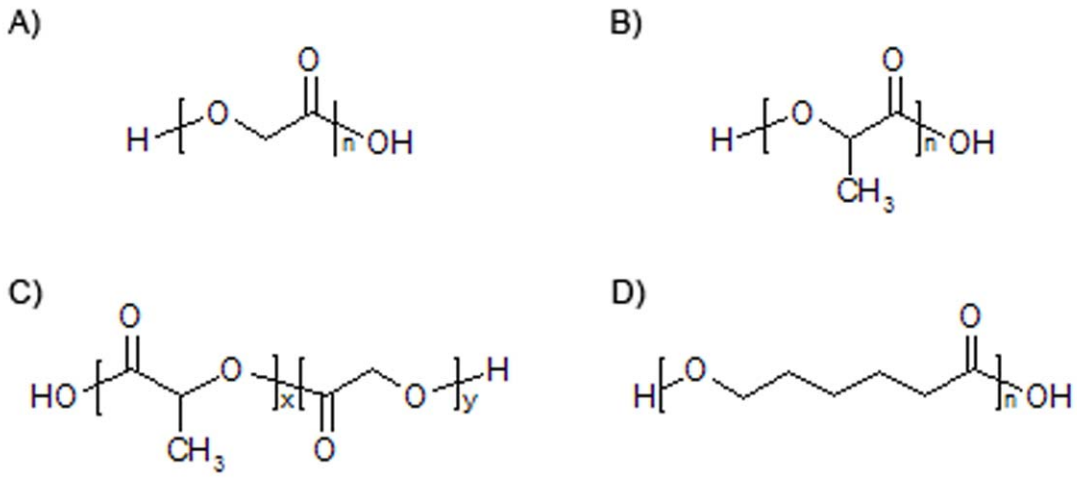

Figure 1.2. A) PGA, B) PLA, C) PLGA and D) polycaprolactone (PCL).

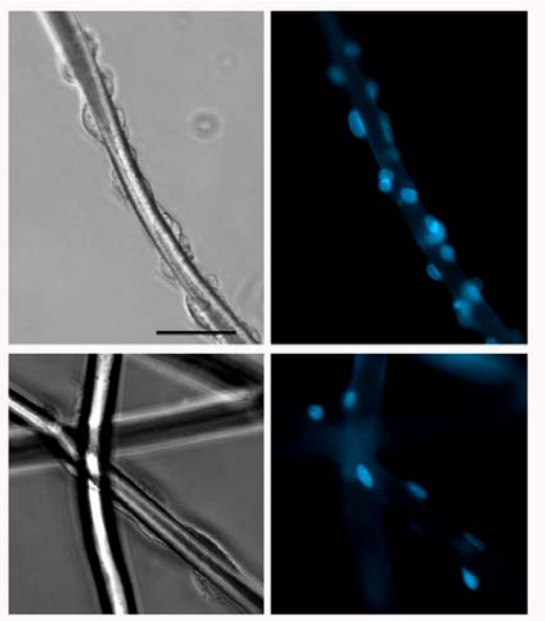

Figure 1.3. Liver-derived stem cell line (Lig-8) cultured on PGA microfibers. Note that cells attached to the surface of the fiber forming a cell monolayer. Scale bar: 100 μm.

Today, many other materials are being designed, synthesized, used and tested in many different presentations such as hydrogels, membranes, foams, nanofibrous scaffolds or sponges for the achievement of every different and specific need. Innumerable synthetic biomaterials are tested everyday, they are designed to be responsive to different stimuli (temperature, pH, electric pulses, molecule-sensitive), to present elastic properties (such as biorubbers) (Lanza *et al*., 2000; Griffith and

Naughton, 2002; Lee and Mooney, 2001), etc… As stated for natural biomaterials, new synthetic biomaterials are under research to design new therapies and launch new products and medical devices into the market.

In the present thesis and within the group of synthetic polymers, the potential of self-assembling peptide hydrogels as scaffolds for tissue engineering and cell culture is described. These peptides are short sequences composed of L-aminoacids, they are easy to synthesize by solid phase synthesis and easy to purify. They are also ideally biodegradable, being the degradation products natural aminoacids, and they have the advantage of having a pore size 1000 times smaller (50-100 nm) than the classic synthetic polymers (PGA, PLA, PGLA). These type of biological materials are composed by repeating units of hydrophilic-hydrophobic aminoacids, in which the charged residues include alternating positive and negative charges. The first molecule of this class, EAK16-II (AEAEAKAKAEAEAKAK, A, alanine; E, glutamine; and K, lysine), a 16 aminoacid peptide, was found as a segment in a yeast protein, zuotin which was originally characterized by binding to left-handed Z-DNA (Zhang *et al*., 1992). Based on this oligopeptide, a large number of self-assembling of ionic self-complementary peptides have been systematically designed by changing the aminoacid sequence and following a periodic pattern. These peptides form β-sheet structures in aqueous solutions and they contain two distinct surfaces, one hydrophobic and the other hydrophilic as it is shown in Figure 1.4. The complementary ionic sides have been classified into several moduli, modulus I, II, IV. For example, modulus I molecules have the following sequence - + - + - +; modulus II, - - + + - - + +; modulus IV, - - - - + + + +. The length, the aminoacid residues and the pattern of the chain can be designed to obtain sequences with different properties (Zhang and Altman, 1999; Caplan *et al*., 2002). This thesis is based on RAD16-I (R arginine, A alanine and D aspartic acid), a peptide included in the modulus I group. The characteristic sequence of these peptides is the responsible for the self-assembling process which is driven by electrophilic and hydrophobic interactions between the peptide molecules (Figure 1.4.). Therefore, these materials self-assemble by stacking of the peptide molecules, forming a network of interweaving nanofibers of 10-20 nm diameter and 50-200 nm pore size (Figure 1.4., Figure 1.5. and Figure 1.6.). By increasing the ionic strength (contacting the peptide with a salt solution or buffer) of the peptide solution the self-assembling process may be accelerated. The peptide solutions form hydrogels of water content higher than 99%, when dissolved in water in a range of 1-10 mg/ml (Zhang *et al*., 1993; Zhang *et al*., 1995; Caplan *et al*., 2000; Holmes *et al*., 2000; Kisiday *et al*., 2002; Caplan *et al*., 2002). Cells encapsulated within these hydrogels experience a truly

three-dimensional environment as it can it shown in Figure 1.3. This class of nanostructured materials better mimics the extracellular matrix (ECM) of the cells compared to other synthetic scaffolds. In contrast to the PGLA scaffolds, same cells loaded into these self-assembling three-dimensional peptide scaffolds, organize in clusters or spheroids, similar to tissue structures found in liver, and acquire hepatocyte phenotype (Figure 1.7., (15)). They also present the advantage in front of the naturally derived polymers of being completely synthetic, feature that allows a control in the composition of the material.

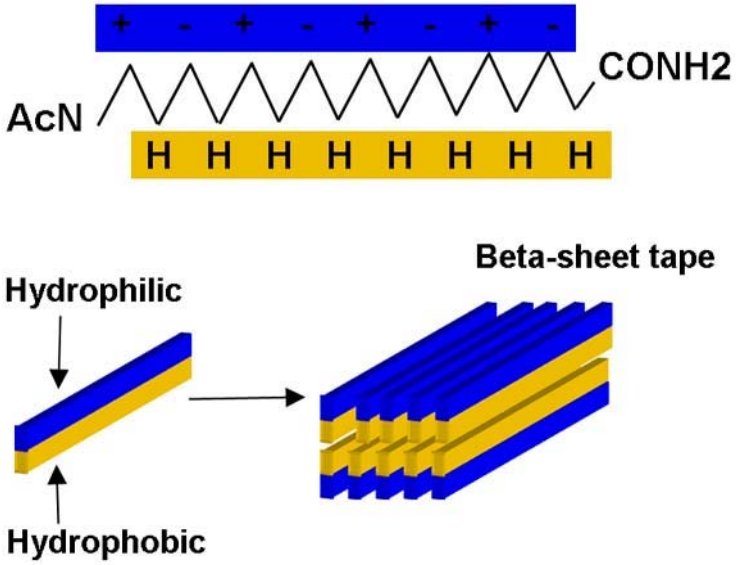

Figure 1.4. Schematic model of the self-assembling process of the modulus I self-complementary peptides.

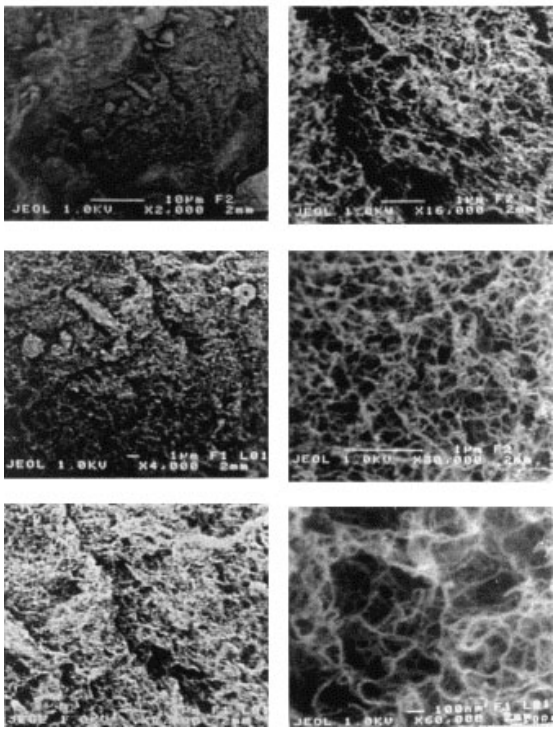

Figure 1.5. Scanning electron microscopy picture of RAD16-II (Holmes,).

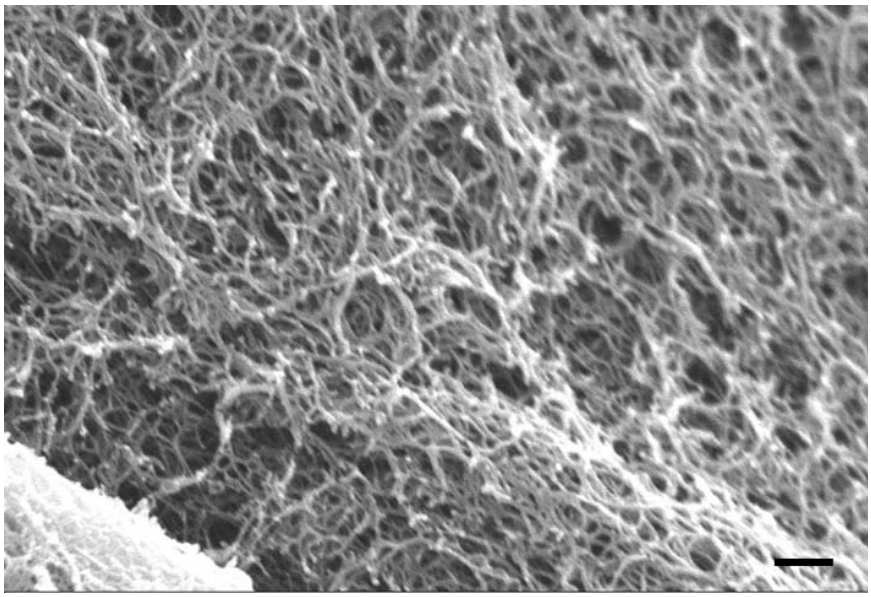

Figure 1.6. Scanning electron microscopy of RAD16-I. Scale bar: 200 nm.

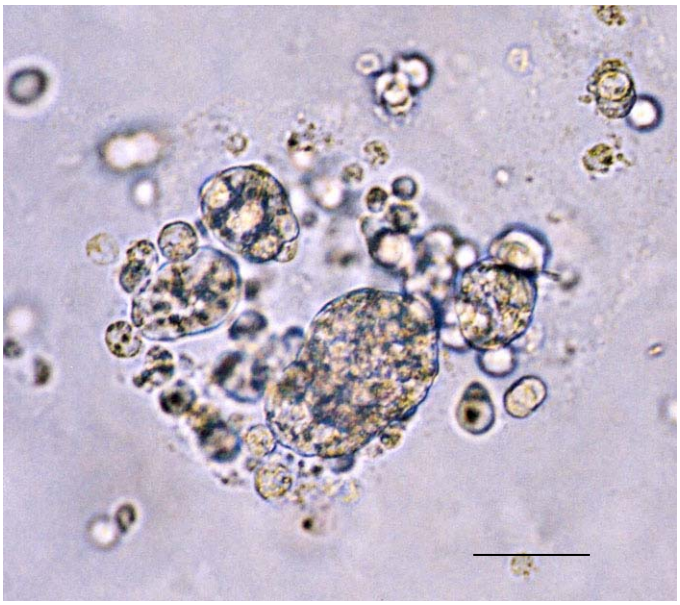

Figure 1.7. Lig-8 cells cultured in a self-assembling peptide scaffold (two weeks). In this case the cells formed clusters or spheroids that acquired hepatocyte phenotype. Scale bar: 100 μm.

As mentioned above, a desirable feature for biomaterials to be applicable in tissue engineering, is the capability for self-assembly into three-dimensional matrices under physiological conditions. The materials presented in this work form a network of nanofibers that mimic the ECM. Normally, animal cells have a diameter between 20-50 μm, thus the three-dimensional peptide scaffold (between 50-200 nm pore size) entraps cells in a truly three-dimensional environment (Figure 1.7.). Other chemical synthetic scaffolds, such as polyglycolic acid (PGA), polylactic acid (PLA) and copolymers of both (PGLA) present fiber networks in the order of 500 μm pore size. In this context, the peptide scaffolds offer a new generation of scaffolds as they entrap cells in a truly three-dimensional matrix in which cells can divide, migrate, and differentiate. It has been shown that some of these peptide scaffolds have the ability to support cell attachment, growth, maintenance and differentiation of a variety of primary and cultured mammalian cells (Zhang *et al*., 1995; Holmes *et al*., 2000; Kisiday *et al*., 2002; Semino *et al*., 2003; Semino *et al*., 2004; Garreta *et al*., 2006). They are clear candidates to use as molecular engineered scaffolds for tissue repair and tissue engineering purposes. Several studies have shown the potential of the self-assembling peptides as scaffolds for tissue repair and regeneration. For example, RAD16-I (AcN-RADARADARADARADA-$CONH_2$) was used as a substrate for extensive mouse neurite outgrowth and active synapse formation (Holmes *et al*., 2000). In another work,

RAD16-I was used as a scaffold in which a putative rat adult liver-derived progenitor cell line (Lig-8) form functional hepatocyte-like spheroid structures. These cells exhibited mature hepatocyte properties when encapsulated in the three-dimensional peptide scaffold (Semino *et al*., 2003).

A different self-assembling peptide scaffold, KLD12 (AcN-KLDLKLDLKLDL-$CONH_2$, K, lysine; L, leucine; and D, aspartic acid), was shown to foster bovine chondrocyte ECM production (Kisiday *et al*., 2002). In this case, the peptide scaffold was used to encapsulate chondrocytes in which they retained their morphology and developed a cartilage-like mechanically functional ECM rich in proteoglycans and type-II collagen, indicative of a stable chondrocyte phenotype. In another study it was used to entrap hippocampal neural cells (Semino *et al*., 2004), and recently the osteogenic differentiation of mouse embryonic stem cells and mouse embryonic fibroblasts when cells were cultured in this scaffold (Garreta *et al*., 2006) was reported.

1.1.3. Cells

An essential requirement in tissue engineering is the use of cells. These cells may be autologous (self) from the patient, allogeneic or xenogeneic. The use of autologous cells has the advantage of presenting minimal risk of immune response and disease transmission. Nevertheless, the main disadvantage of the use of autologous cells is that it does not allow off-the-shelf availability of the engineered tissue. The alternative relays on the use of allogeneic cells from a human donor who is not immunologically identical to the patient, and xenogeneic cells from different animal species. This last case remains controversial because of the potential of transmitting animal pathogens to humans. Cells can also be stem cells, that are capable to self-renew and differentiate into a variety of cell lineages, or differentiated cells at different stages of maturation (Griffith and Naughton, 2002).

The most accepted definition for a stem cells is that of a cell that has the capacity for self-renewal and is capable of forming at least one, and some times many, specialized cell types through differentiation (Marshak *et al*., 2001). Usually, between the stem cell and its differentiated progeny there is an intermediate population of commited progenitors with limited self-renewing capacity and restricted differentiation potential (Watt and Hogan, 2000) (Figure 1.8.).

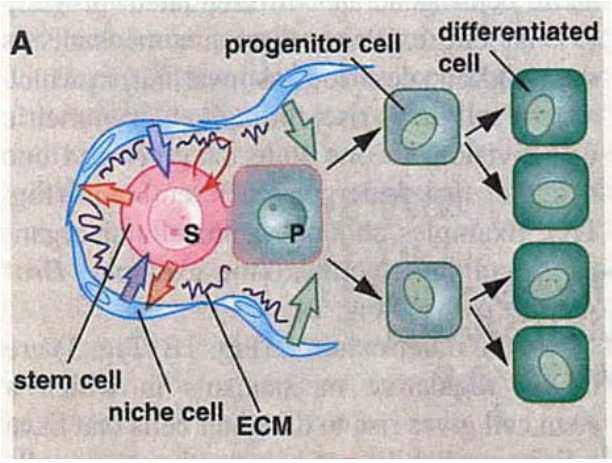

Figure 1.8. Prototypic adult stem cell compartment. Stem cell (S) surrounded by niche cells (blue cells), soluble factors and extracellular matrix components (ECM) forming the microenvironment. In this context, stem cells divide asymmetrically to self-renew and produce one progenitor cell (P) that is instructed by the new environment (green arrows). The progenitor cells divide exponentially to expand and produce final differentiated cells (functional tissue cells, dark green) (Watt and Hogan, 2000).

Stem cells may be isolated either from embryos, from umbilical cords or from adult tissues. The potential medical use of stem cells, including tissue engineering is very exciting, although the use of human embryonic and fetal stem cells is a field full of controversy and ethical concern. It has to be taken in to account the recent efforts and research in the field that no embryos are destroyed. There are recent publications (Chung *et al*., 2006; Klimanskaya *et al*., 2006) in which mice (Chung *et al*., 2006) and human (Klimanskaya *et al*., 2006) embryonic stem cells (ESC) are derived without the need of destroying the embryo by extracting and expanding a single blastomere in the 8-10 cell stage stage of development. Leaving this debate aside, embryonic and adult stem cells differ, for example in the number of types of differentiated cells that can be derived from them (Donovan and Gearhart, 2001). Embryo-derived stem cells are thought to be pluripotent, that means that theoretically they can give rise to almost every cell type, while adult stem cells are thought to be multipotent, that is, they can differentiate into a limited number of cells. However, ESC present the disadvantage that they may be tumorigenic due to their highly proliferative state when undifferentiated (Cai *et al*., 2004; Baker *et al*., 2007).

Other differences exist between both types of stem cells. For example, *in vitro* cultures of mouse embryonic stem cells have been established indefinitely without losing differentiation potential, by culturing the cells in the presence of leukemia

inhibitory factor (LIF) and feeder layers of mouse embryonic fibroblasts (MEF), but similar conditions have not been found for adult stem cells. It is difficult to propagate and expand *in vitro* functional adult stem cells, therefore this is one of their main limitations for their application in biomedical technologies. A typical example is the hematopoietic system, which are not possible yet to expand in culture without losing differentiation potential (Weissman, 2000). Therefore, extensive research in designing protocols and methods are needed to stabilize and expand adult stem cells.

Once a type of cell to use for research is chosen, either mature or stem cell, the next step consists on its manipulation to obtain the desired behavior. One interesting and used approach to manipulate the cell function is by modifying its microenvironment (Klimanskaya *et al*., 2006; Weissman, 2000).

1.1.4. General hypotheses: regulation of the cell microenvironment

The general hypothesis in which this work is based on, is the regulation of the extracellular microenvironment. This microenvironment in which the cell lives, which is the result of the combination of the extracellular matrix, physicochemical environmental cues and cell-cell interactions, controls cell fate. Manipulating the cell microenvironment normally leads to a change in cell function. Therefore a widely strategy used in tissue engineering is the addition of physicochemical and mechanical signals to an *in vitro* system, in order to control and regulate cell function, differentiation and to obtain a desired functional response. These aspects interact synergistically *in vivo* to regulate and control cell fate, and will be applied to different *in vitro* systems to obtain a *in vivo*-like cellular response.

One first step in order to achieve these goals is the selection of a suitable scaffold or biomaterial that imitates the natural extracellular matrix of the cell. As mentioned above, the scaffold has to be a highly porous extracellular matrix analog capable to sustain and guide cell growth. In this sense, the self-assembling peptide scaffolds presented in this work meet most of the necessary requirements to be suitable scaffolds for cell culture. These materials can be functionalized with signaling molecules (peptides, carbohydrates, lipids,..) that confer instructive features to the scaffold.

Moreover, and as stated above, cells respond to the extracellular environment by sensing a chemical signal or physical/mechanical stimulus. These signals are transmitted to the nucleus to trigger the expression or repression of genes, the

products of which regulate cell division, migration, differentiation and apoptosis (Sipe, 2002). The extracellular environment in terms of soluble factors or mechanical forces may also be modified to tune cell function and differentiation. Soluble factors such as growth factors, drugs or chemical compounds may be added to the culture medium, in order to promote a determined behavior (Griffith and Naughton, 2002; Griffith and Swartz, 2006; LeCluyse *et al*., 1996). Mechanical forces, which can influence cell shape, gene expression and metabolic pathways, are normally applied to the cultures using bioreactors (Powers *et al*., 2002; Schmitmeier *et al*., 2006; Semino *et al*., 2006).

1.1.5. Motivation and objectives of the present work

The motivation of the present work is to provide functionalized and unique specific microenvironments to the cells with the purpose of improving and modulating adult cell function and promoting stem cell differentiation. The final application would be to use these new class of biomaterials for pharmaceutical diagnostics, medical devices and regenerative medicine.

The objectives of this Thesis are:

1. Design and characterization of novel tailor-made self-assembling peptide scaffolds which better mimic the extracellular environment (Chapter 2).
2. Study and characterize the protease degradability of RAD16-I peptide scaffold (Chapter 3).
3. Study endothelial cell monolayer formation, differential proliferation and function on the new functionalized self-assembling peptide scaffolds in comparison to cells grown in regular culture dishes (Chapter 4).
4. Build a synthetic *in vitro* hepatocyte culture system capable of the maintenance of liver-specific gene expression and function (Chapter 5).
5. Study the differentiation of an adult liver putative progenitor cell line, Lig-8 in the self-assembling peptide scaffold (Chapter 6).

Chapter 2: *Design and characterization of novel tailor-made self-assembling peptide scaffolds*

2.1. INTRODUCTION: Recreating microenvironments

It has already been mentioned in Chapter 1 that the microenvironment that surround the cells is composed of the ECM, cell-ECM contacts, cell-cell contacts as well as soluble factors and biophysical parameters such as mechanical forces, temperature, pH, etc... Following the general hypotheses of the Thesis, novel biomimetic materials focused on the ECM of the cells were designed. The peptide scaffolds designed in this part of the work are based on RAD16-I self-assembling peptide. It was decided to functionalize this three-dimensional peptide scaffold in order to give the cell a microenvironment that better recreates the extracellular matrix (ECM) and ensures proper cell maintenance and function.

The cellular ECM is a three-dimensional network mainly composed by laminins, collagens, and proteoglycans (Figure 2.1.). It is not only important as a structural component, supporting cell attachment and providing boundaries between tissues and organs, but it also gives the cells an instructive microenvironment that dynamically interacts with them and modulates their function. Indeed, short peptide sequences present in proteins of the basement membrane (BM) have been identified to participate in series of important biological functions including cell attachment, proliferation, differentiation and migration (Iwamoto *et al*., 1987; Kleinman *et al*., 1989; Koliakos *et al*., 1989; Skubitz *et al*., 1990; Tsilibary *et al*., 1990; Sakamoto *et al*., 1991).

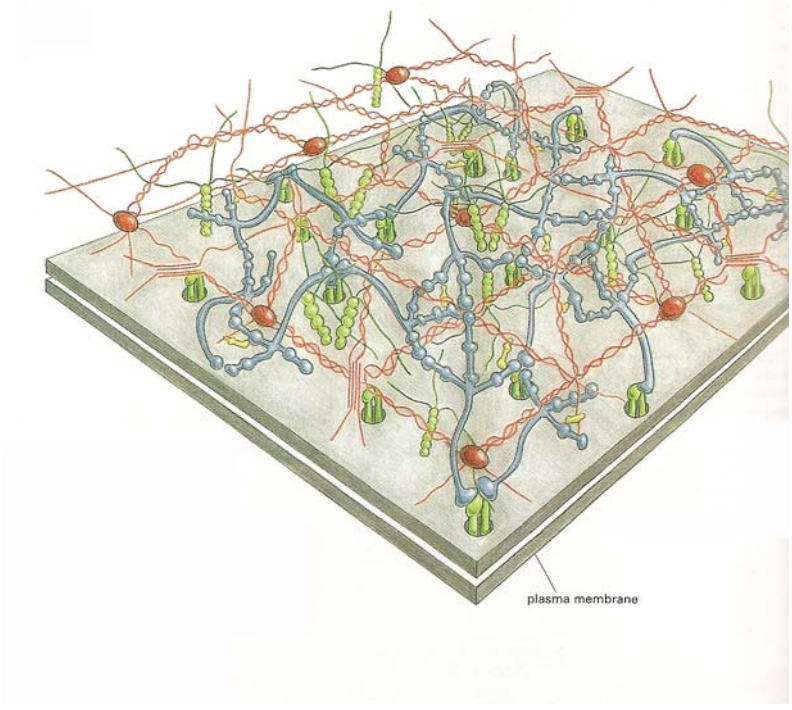

Figure 2.1. Scheme of the extracellular matrix showing different components. Blue: Laminin, Red: Collagen IV, yellow: nidogen, green: perlecan.

In order to obtain synthetic ECM or basement membrane analogs, new biologically inspired peptide scaffolds were designed by functionalization of the self-assembling peptide RAD16-I (prototypic peptide) with additional sequences involved in cell attachment and function (Table 2.1.) (Semino, 2003). This approach has been previously used in other studies in which a signalling peptide or biologically active molecule is coupled to the biomaterial in order to obtain functionalized scaffolds (Genove *et al*., 2005). For example, Stupp *et al.* (Silva *et al*., 2004) reported the neural progenitor cell differentiation into neurons when encapsulated in a peptidic hydrogel containing the neurite promoting laminin epitope IKVAV. In another study Lutolf and colleagues designed PEG hydrogels with cell-adhesive properties, containing the RGD peptide sequence (Lutolf *et al*., 2003).

Similarly, new peptide sequences were synthesized by extension of the RAD16-I peptide at the amino terminal. In order to keep the active sequence free, two glycines between the main chain and the new sequence were added as spacers. The generic sequence therefore obtained was AcN-X-GG-$(RADA)_4$-$CONH_2$, being X the sequences shown in Table 2.1. A complete description of each sequence can be found in Table 2.2. In addition, a three code letter name was given to each peptide as an abbreviation to simplify the nomenclature (Table 2.2).

At the time the peptides were designed, it was hypothesized that similarly to RAD16-I, the novel functionalized peptides would also undergo a self-assembling process, forming a network of nanofibers and leaving the biological active motif available as a signaling sequence that would promote a specific biological function. For the purpose of building a synthetic basement membrane and following a biomimetic approach, the novel tailored peptides were designed with the intention to be blended in different proportions with the prototypic RAD16-I (Figure 2.2. and Figure 2.3.), as there is a determined amount of the biological active sequences in the extracellular matrix. In the present work, the ability of these new compounds to solubilize in water, to self-assemble into a three-dimensional network of nanofibers and to form hydrogels was tested (Genove *et al*., 2005). In addition the mechanical properties were compared to those of RAD16-I. Differences in the physicochemical, structural and self-assembling properties were expected, as the extentions ranged from the addition of 7 aminoacids to doubling the length of the peptide (Genove *et al*., 2005).

Table 2.1. Peptide sequences from basement membrane proteins and their biological activities

Peptide sequence	Protein	Biological activity
AASIKVAVSADR	Laminin-1	Neurite extension in PC12 cells
CSRARKQAASIKVAVSADR	Laminin-1	Degradation of Matrigel matrix, endothelial mobilization, capillary branching, vessel formation (*in vivo*)
YIGSR	Laminin-1	Cell adhesion, cell migration, endothelial tubular formation
PDGSR	Laminin-1	Cell adhesion
RYVVLPR	Laminin-1	Cell adhesion
KAFDITYVRLKF	Laminin-1	Endothelial cell adhesion and tubular formation, neurite outgrowth
TAGSCLRKFSTM	Collagen-IV	Binds to heparin and heparan sulphate, promotes adhesion and spreading of bovine aortic endothelial cells

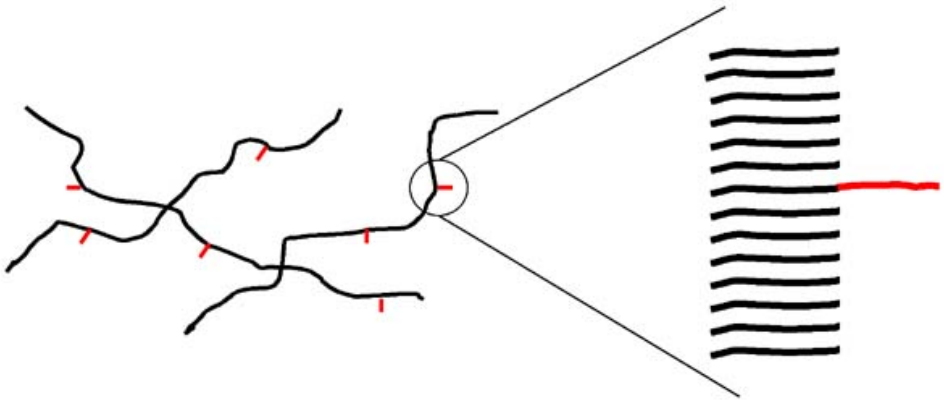

Figure 2.2. Schematic representation of a generic self-assembling peptide hydrogel network (black lines) blended with a functionalized peptide (red lines) with the added sequences extending from the amino terminal. Close up: stacked self-assembling peptide nanofiber (black lines) and the extended sequence of the peptide motif at the amino terminal of one of the sequences (red line).

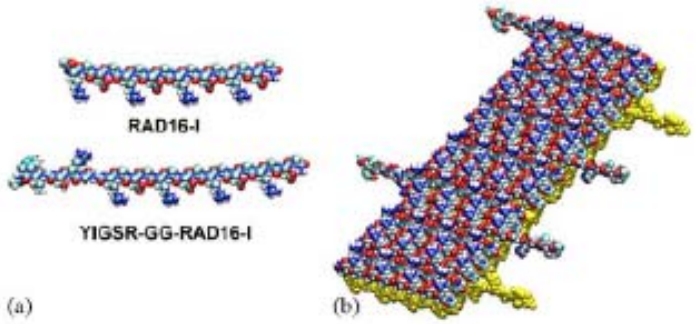

Figure 2.3. Molecular models of self-assembling peptide scaffolds. A) represents the peptide RAD16-I (top) and YIG (bottom). B) Model representing a double β-sheet tape of a self-assembled peptide nanofiber of a mix composed of peptide RAD16-I:YIG (9:1). Note the sequences YIGSR extending out of the nanofiber tape (Genove *et al*., 2005).

2.2. RESULTS

Table 2.2. summarizes the physicochemical and structural properties found for RAD16-I and the modified peptide scaffolds. To simplify the nomenclature of each designed peptide, an abbreviation is given for each peptide (Genove *et al*., 2005).

Table 2.2. Physicochemical and structural properties of peptide scaffolds used.

Name	Peptide sequence	Solubility in water 1% (w/v)	Gel formation (visual)	Secondary structure (CD)	Presence of nanofibers (AFM)
RAD16-I	AcN-$(RADA)_4$-$CONH_2$	+	+	β-sheet	+
AAS	AcN-AASIKVAV-GG-$(RADA)_4$-$CONH_2$	+	+	β-sheet	+
CSR	AcN-CSRARKQAASIKVAV-GG-$(RADA)_4$-$CONH_2$	-			
YIG	AcN-YIGSR-GG-$(RADA)_4$-$CONH_2$	+	+	β-sheet	+
PDS	AcN-PDSGR-GG-$(RADA)_4$-$CONH_2$	+	+	β-sheet	+
RYV	AcN-RYVVLPR-GG-$(RADA)_4$-$CONH_2$	+	+	β-sheet	+
KAF	AcN-KAFDITYVRLKF-GG-$(RADA)_4$-$CONH_2$	+	+	β-sheet	-/+*
TAG	AcN-TAGSCLRKFSTM-GG-$(RADA)_4$-$CONH_2$	+	+	β-sheet	+

* Short nanofibers were observed

First, the solubility of the new functionalized peptide scaffolds in water was tested at the same concentrations in which RAD16-I is normally prepared. All the sequences were found to form clear solutions in water at a concentration of 1% (w/v, 10 mg/ml) except for CSR which was insoluble (see Table 2.2). This last functionalized peptide was not used for the next series of assays.

In addition, each peptide solution at 1% was used to assess hydrogel formation. All the assays were always performed side to side with RAD16-I at 1% as a control. In two cases, the control peptide (RAD16-I) and one of the functionalized sequences (AAS), an increase in the viscosity of the solution after they were left standing overnight at room temperature was observed, simply by visual inspection. Longer periods of time (aproximately 2 days) were required to observe an increase in the viscosity for the rest of the functionalized peptides. Moreover, hydrogel formation was rapidly induced by getting in contact the peptide solution with phosphate buffer saline (PBS) through a porous membrane (Materials and Methods, section 7.3.2), as it is observed also for the prototypic peptide RAD16-I.

Furthermore, circular dichroism studies were performed in order to assess the secondary structure of the novel peptides. Circular dichroism (CD) is a spectroscopic technique very useful to study protein structures, from secondary structure to tertiary structure as well as protein-protein interactions. The secondary structure identifies ordered structures within a polypeptide such as α-helices and β-sheets, or polypeptides without a concrete ordered structure (random coil). The tertiary structure of a protein defines the overall 3-D structure of a folded protein, which conferes the protein its functions. The far UV zone of the CD spectra (190-250 nm) is useful in the detection of secondary structures, while the near UV zone of the spectra (250-350) is used to detect changes in tertiary structures. A typical CD spectrum for a β-sheet structure shows a minimum molar ellipticity around 218 nm, which represents the β-sheet content and a maximum at 195 nm which corresponds to the backbone twist of the peptide in β-sheet configuration. The CD spectrum for a α-helix shows two minimums at 209 and 222 nm (Havel, 1996) whereas random coil peptides or proteins are represented by a strong minimun in the 190-200 nm range (Figure 2.4.). RAD16-I is known to present a β-sheet secondary structure. The secondary structure of the designed peptides was studied in a similar way in order to elucidate whether the addition of the functionalization affected the β-sheet secondary structure, and thus the self-assembling of the peptide molecules.

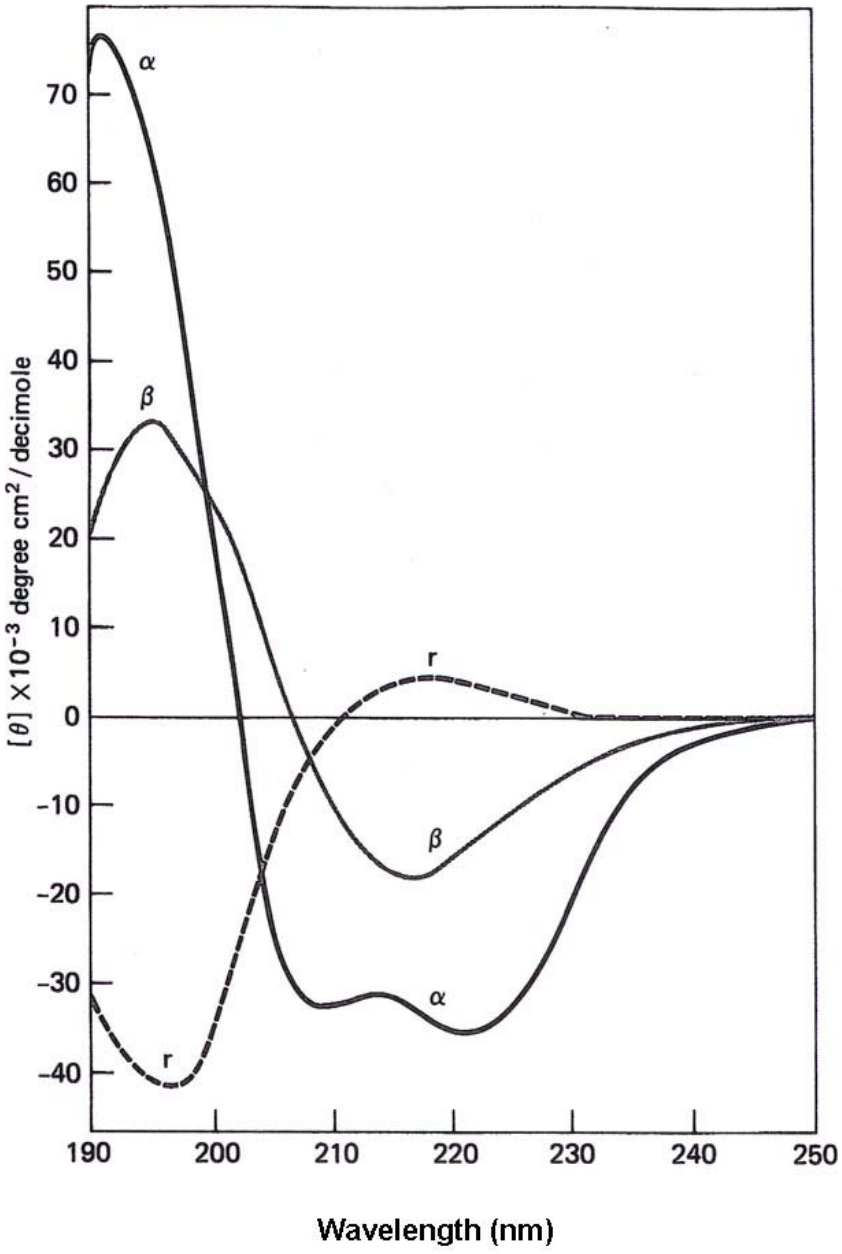

Figure 2.4. CD spectra of poly(Lys) in the α-helical (α), β-sheet (β), and random coil (r) conformations (Greenfield and Fasman, 1969).

CD studies for all of the functionalized peptides showed a spectrum indicative of β-sheet structure with a minimum molar ellipticity (degcm^2/decimole) around 216 nm (Figure 2.5.). The observed secondary structures are enlisted in Table 2.2. We observed that the addition of the short peptide sequence was translated into weaker β-sheet structures, as shown by a decrease in the intensity of molar ellipticity at 216 nm

(Figure 2.5). The addition of at least 7 aminoacids up to 15 aminoacids (Table 2.2.) in the functionalized sequences, added to the fact that these sequences don't follow anymore the repetitive and characteristic sequence of alternating hydrophilic-hydrophobic aminoacids, results (as predicted) in a decrease of the self-assembling of the peptide molecules (Genove *et al*., 2005).

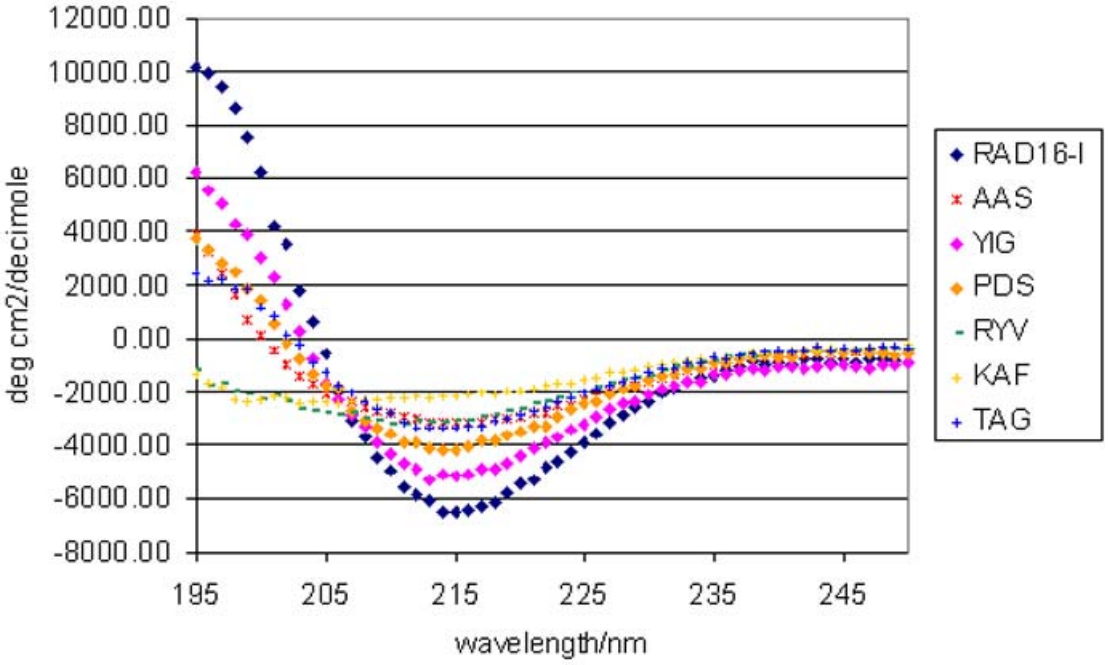

Figure 2.5. CD spectra of peptide scaffolds. Peptides were diluted from stock solutions at a final concentration of 25 μM. Abbreviations are indicated in Table 2.2. All peptide show β-sheet structute with different β-sheet (216 nm) content and backbone twist (195 nm).

In addition, Atomic Force Microscopy (AFM) was used to detect the presence of nanofibers formed by a peptide self-assembling process. AFM is a technique that provides high resolution of surface structures down to the nanometer scale by measuring the interaction of a microscopic sharp tip used to scan the sample surface, and the sample. AFM consists of scanning a sharp tip on the end of a flexible cantilever across a sample surface while maintaining a small, constant force. The scanning motion is conducted by a piezoelectric tube scanner which scans the tip in a raster pattern with respect to the sample (or scans to the sample with respect to the tip). The tip-sample interaction is monitored by a reflecting laser off the back of the cantilever into a split photodiode detector. By detecting the difference in the photodetector output voltages, changes in the cantilever deflection or oscillation amplitude are determined (Russell *et al*., 2001). There are two most commonly used modes of operation: contact mode AFM and Tapping Mode AFM which are conducted in air or liquid environments. Contact mode AFM operates by measuring repulsive forces between a tip and the sample (Binning *et al*., 1986). The instrument lightly touches the tip. In Tapping Mode AFM, the images are derived from measurements of attractive forces, the tip does not touch the sample. It oscillates at its resonance frequency lightly "tapping" on the surface during scanning.

In the present Thesis Tapping Mode AFM was used because it allows to measure soft, fragile, and adhesive surfaces without damaging them which can represent a drawback for contact mode AFM. The samples were prepared by diluting the stock peptide solution (1:100) in deionized water in order to clearly observe the presence or not of nanofibers. Our previous experience imaging RAD16-I peptide nanofibers under the AFM, taught us that higher concentrations presented an enourmous amount of nanofibers leading to poor imaging. Figure 2.6. shows AFM images for the prototypic RAD16-I. Nanofibers can be observed in the image which represents an area of 1 μm x 1 μm (Scale bar 250 nm). Many nanofibers were observed for all new peptide sequences except for KAF. In this case, there were few and short nanofibers, probably due to the high hydrophobic residue content which might distort the self-assembling portion of the sequence confirmed in part by the low β-sheet content observed by CD (Figure 2.5, Figure 2.6., F) (Genove *et al*., 2005).

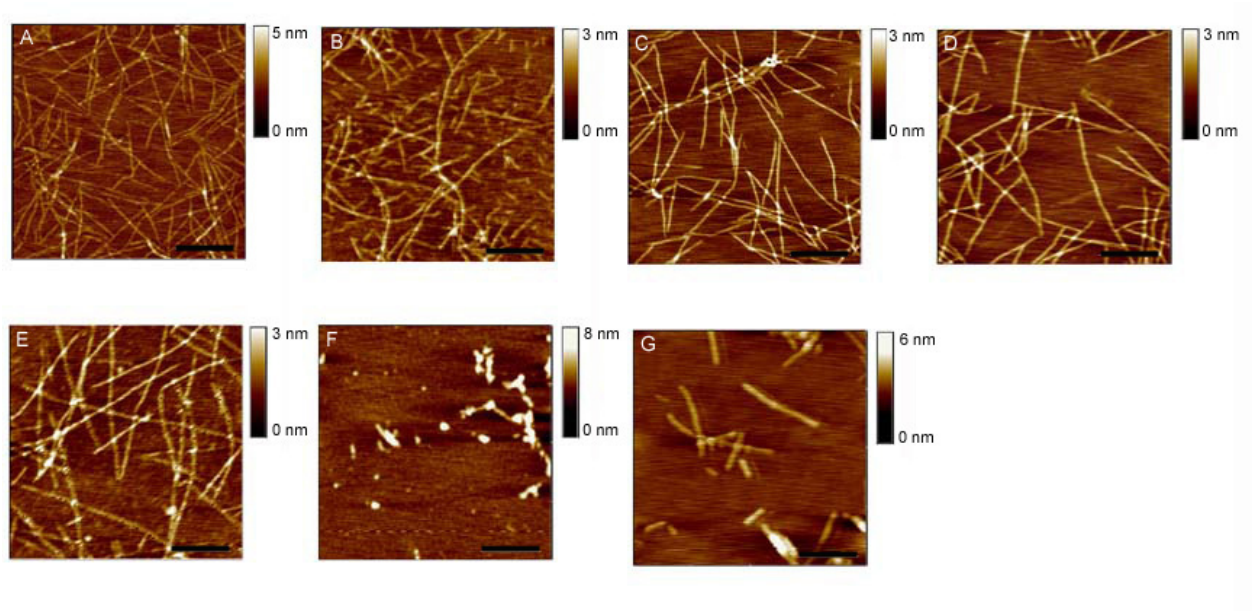

Figure 2.6. AFM images of RAD16-I and functionalized peptide nanofibers at a final concentration of 0.01% (w/v). A) RAD16-I, B) AAS, C) YIG, D) PDS, E) RYV, F) KAF and G) TAG. Scale bar: 250 nm.

Furthermore, in order to test the vicoelastic properties of the peptide scaffolds rheological assays were performed. Oscillatory rheometry was used, which subjects samples to oscillating stresses or oscillating strains. The experiments were carried out using a controlled strain rheometer, which shears the sample at a controlled strain within a range of frequencies and gives G*, the complex modulus, as an output. This complex modulus can be defined as:

$$G^* = G' + iG'' \qquad \text{[eq. 2.1]}$$

Where G' is the storage modulus which represents the elastic/solid character of the material, and G'' is the loss modulus which represents the viscous/fluid character of the material.

In oscillatory rheometry, for a viscous solution, the viscous component of the complex modulus, the loss modulus (G'') decreases with decreasing oscillatory frequencies, and the storage modulus G' is low. For gels, G' and G'' are relatively constant with oscillatory frequency, and G' is much greater than zero (Kavanagh and Ross-Murphy, 1998).

Firstly, a dynamic strain sweep was on RAD16-I peptide was performed (Figure 2.7.) to set the linear viscoelastic region of the test and to select a fixed strain for the dynamic frequency sweep tests. This linear viscoelastic range is defined by constant moduli, G' and G". It is important to select a strain within this range to further obtain reliable results (Schramm, 1994). The strain selected was 0.01 (dimensionless) and was applied in all assays.

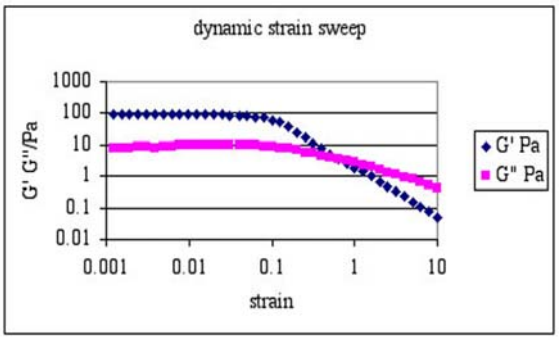

Figure 2.7. Dynamic strain sweep test performed for RAD16-I.

Then, an oscillatory rheometric test was performed using RAD16-I at 0.5% in water (Figure 2.8., A). It can be observed that RAD16-I presented a gel-like pattern with G'>G'' and constant along the range of frequencies tested. After performing a test for RAD16-I in its liquid form, PBS was added around the plates for 10 min to induce hydrogel formation, and the test was performed once again. Figure 2.8., panel B shows the results obtained for this experiment. Although before adding PBS the peptide RAD16-I was already a gel (G'>G" and constant moduli), upon the addition of salts both moduli increased (~10 fold), indicative of a significant increase of gel strength (Genove *et al*., 2005).

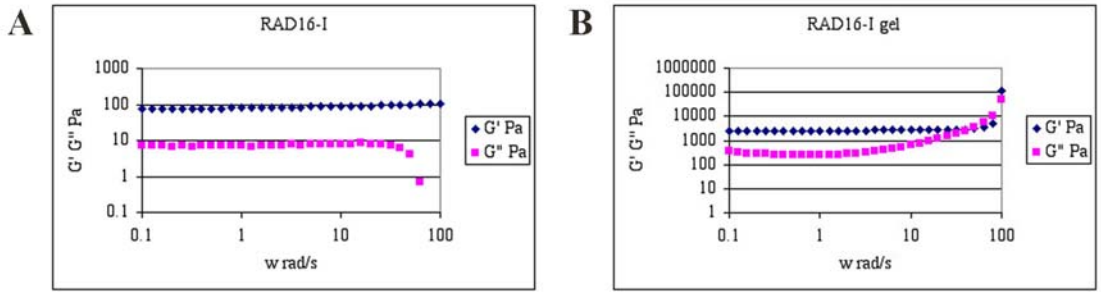

Figure 2.8. Comparison of dynamic frequency sweep tests for RAD16-I A) before the addition of PBS, B) after a 10 min incubation in contact with PBS.

For the functionalized sequences, assays were performed after the incubation in contact with PBS. Results from rheological measurements of all peptides are shown in Figure 3.8. As in the case of RAD16-I, G' is greater than G'', indicative of a gel-like profile. In the case of the prototypic sequence RAD16-I the value of the storage modulus G' reaches $2.5x10^3$ Pa (Figure 2.9.) whereas the magnitude for the peptide AAS is about 10 times lower ($1.5x10^2$ Pa), and 100 times lower for the rest of the sequences (Figure 2.9.). These results show that the addition of a sequence interferes with the self-assembling process which may be due to a possible distortion of the β-sheet configuration of RAD16-I (see Figure 2.5.). The fact that a gel behavior is observed by rheometrical assays also confirms the visual observation of gel formation (Table 2.2) and the reduced β-sheet configuration as it was seen in Figure 2.5. (Genove *et al*., 2005)

In Figure 2.9 the behavior of the different peptide sequences with time is shown. At the selected frequency (10 rad/s), both moduli G' and G'' remain constant with time, indicating that each gel has reached equilibrium with the buffer solution mantaining stable rheological properties (Genove *et al*., 2005).

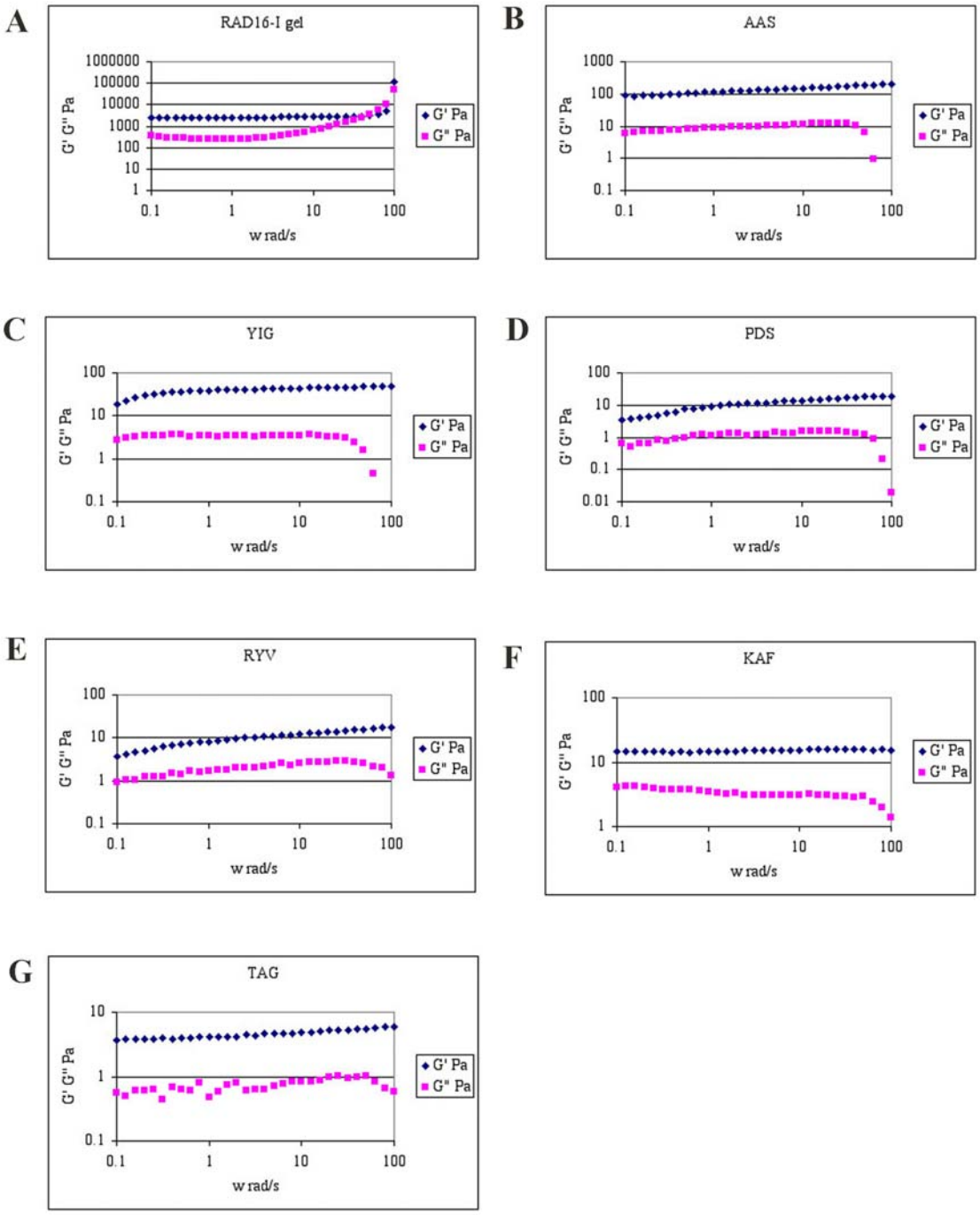

Figure 2.9. Dynamic frequency sweep test for peptide scaffolds at a a fixed strain of 0.01. A) RAD16-I, B) AAS, C) YIG, D) PDS, E) RYV, F) KAF, G) TAG. G' (Storage modulus) represents the elastic character of the material, and G" (Loss modulus) represents its viscous character.

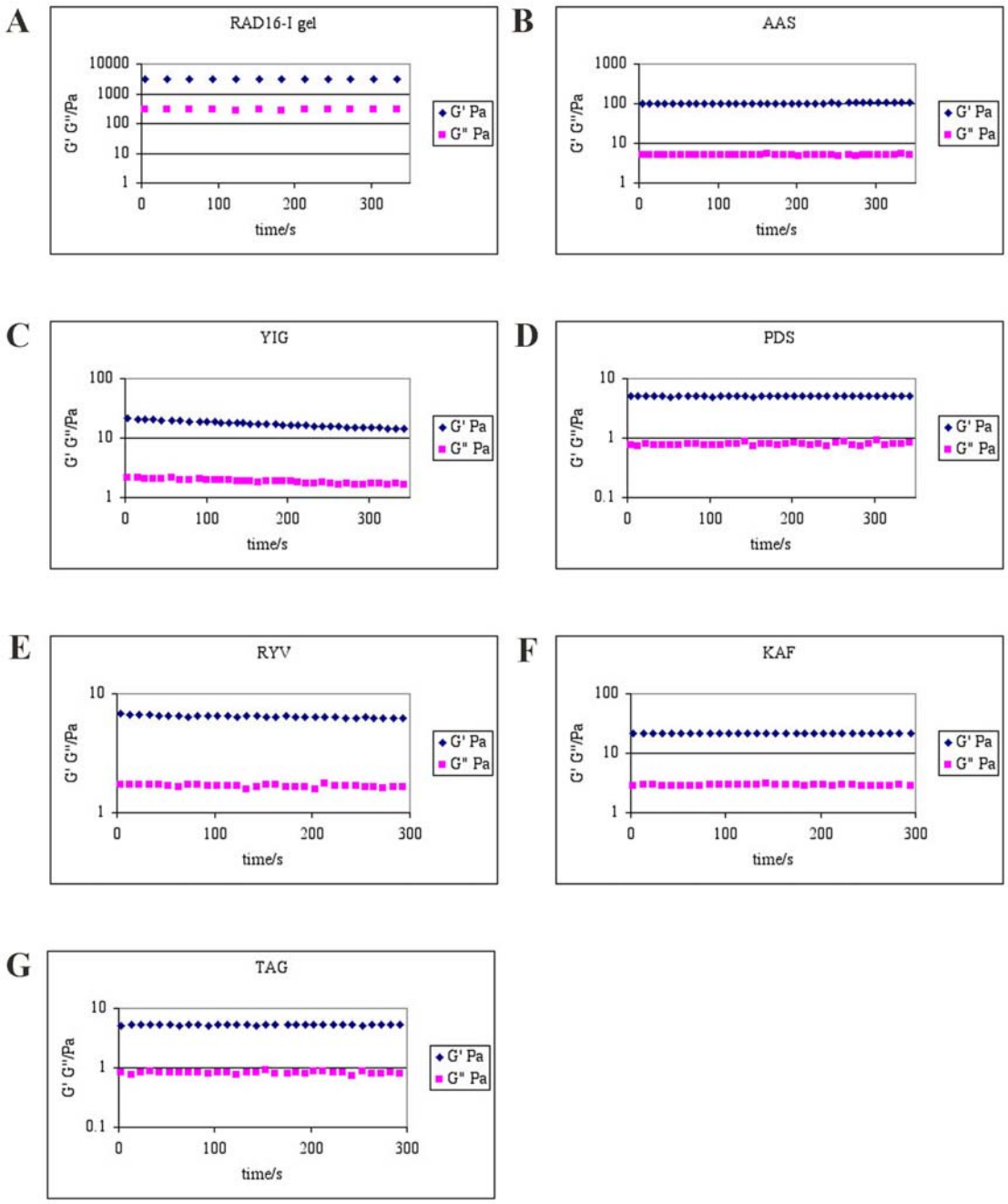

Figure 2.10. Dynamic time sweep test for peptide scaffolds at a fixed frequency of 10 rad/s. A) RAD16-I, B) AAS, C) YIG, D) PDS, E) RYV, F) KAF, G) TAG.

2.3. DISCUSSION

The self-assembling peptide hydrogel RAD16-I was functionalized in order to obtain extracellular matrix analogs. The new peptide scaffolds were tailored by extending the RAD16-I peptide sequence at the amino-terminal with laminin-1 and collagen-IV motifs, two of the main proteins from de basement membrane. The chosen peptide sequences are shown in Table 2.2. The structural properties of the new functionalized peptides were studied to determine the capacity to form hydrogels. Changes in the β-sheet structure as well in the capacity to form hydrogels and nanofibers were expected, due to the length of the peptide sequence added, as well as to the distortion of the repetitive hydrophilic-hydrophobic nature of the RAD16-I peptide hydrogel. In fact, those parameters were affected in the new functionalized peptides resulting in hydrogels with weaker β-sheet structure, as shown by a decrease in the intensity of molar residue ellipticity at 216 nm (Figure 2.5.). Moreover, a change in the viscoelastic properties was observed; for instance, the storage modulus G' in the RAD16-I hydrogel reaches $2.5 \cdot 10^3$ Pa, but the magnitude of G' for the functionalized peptides is in a range from 10 to 1000 times lower. Nevertheless, the rheometric profile indicates that the peptides form gels, as indicated by G'>G'' and both constant along the range of frequencies tested.

We have developed what we consider a new generation of the self-assembling peptides, containing biological active sequences from laminin-1 and collagen IV. These materials will be tested to be cell-responsive and presumably, they will be useful in diverse areas of biomedical research. In our case, we have tested the capacity of a functionalized set of self-assembling peptides to instruct endothelial monolayer development and function as wel as maintenance of rat hepatocytes liver specific functions (see Chapter 4 and 5, respectively). Moreover, this system represents a very interesting platform to obtain an innumerable amount of functionalized biomaterials promoting different biological activities. In a similar manner, RAD16-I may also be functionalized with other biomolecules, such as sugars, lipids, etc… widening the spectrum of activities. The blending process of the functionalized peptides in the prototypic RAD16-I matrix, allows to incorporate many different motifs very easily, making it possible to build complex extracellular matrix analogs.

Chapter 3: *Protease degradation of RAD16-I peptide scaffold*

3.1. INTRODUCTION

Tissue engineering and regenerative medicine require biomaterials capable to maintain and guide cell growth, migration, differentiation and function. These materials should be highly porous natural or synthetic scaffolds that mimick the extracellular matrix (ECM), and should allow diffusion of nutrients, oxigen and metabolic waste products. In addition the scaffold should work just as a temporal support, and ideally it would be gradually degraded while cells build their own ECM. Generally, naturally derived scaffolds present the advantage to resemble the extracellular matrix found *in vivo*, they present biological binding sites, and also they are susceptible of degradability by secreted proteases of the cells, allowing both ECM turnover and cell migration within the scaffold. However, as mentioned in Chapter 1, they present other limitations as the batch to batch variations, and the possibility that they may carry pathogens from other species. They might also be extremely instructive providing too much signalling to the cells which in some applications might be a drawback as they could induce undesired differentiation programmes. Thus, there is a important effort and progress in designing and synthesizing completely defined materials that more and more mimick the complexity of the ECM, in terms of structure, cellular biorecognition and function, and degradability specific for each tissue of interest (Lutolf and Hubbell, 2005).

As it is depicted in Figure 3.1. there are several options and ways to address the obtantion of a ECM analog. Biologically-active peptide sequences which can be cell-adhesive ligands, degradation domains for proteases, a binding site for a specific growth factor or either a growth factor *per se*, are either synthesized or obtained by recombinant engineering technologies and cross-linked to the polymer or biomaterial of interest. Then, the polymer is cross-linked to obtain a three-dimensional designed ECM analog. To assess this final cross-linking there are many approaches, for example, nano-fibrillar networks can be obtained by self-assembly of amphiphilic molecules driven by electrostatic and hydrophobic interactions, which is the case of RAD16-I, the peptidic biomaterial on which this Thesis is based. Another possibility is to covalently cross-link the polymer chains taking advantage of its chemistry using chemical reactions, photopolimerization processess, and so on.

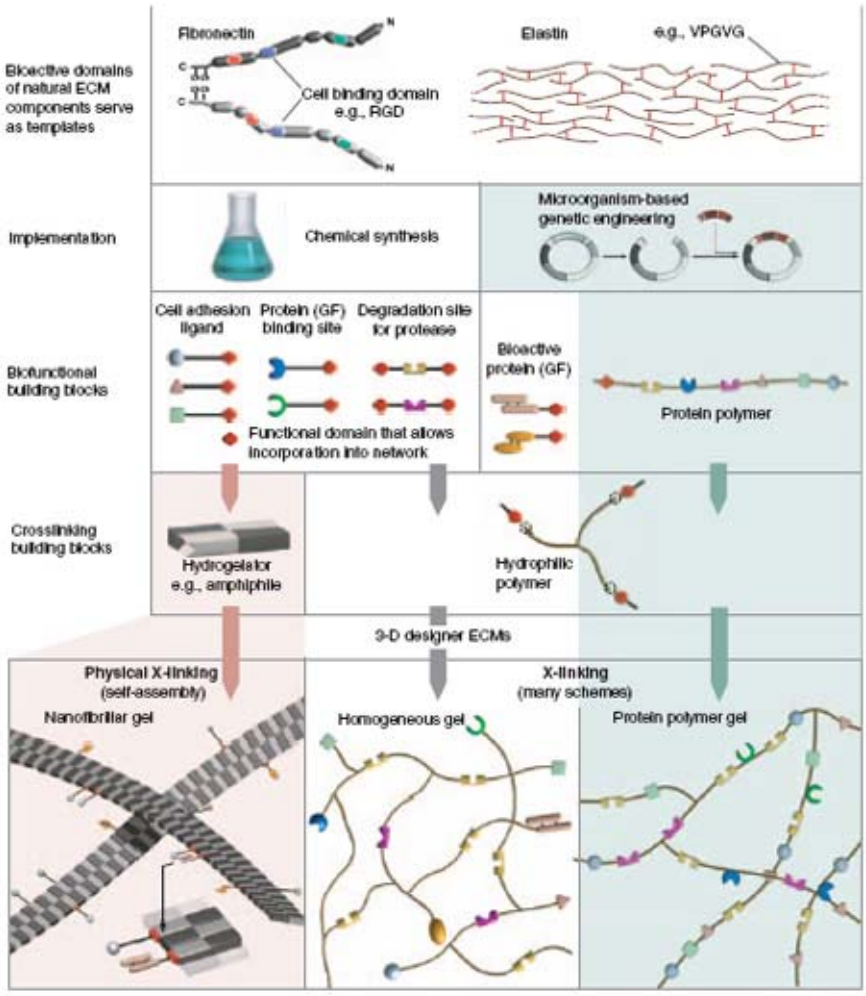

Figure 3.1. Design strategies addressed to obtain taylor-made synthetic ECM analogs that mimick the ECM complexity (Lutolf and Hubbell, 2005).

Regarding to the biodegradation of the scaffold, many synthetic biomaterials have been designed to present degradation by ester hydrolysis, which is in contrast with the *in vivo* ECM turnover, degraded and remodeled by proteases mainly matrix metalloproteases (MMP) and serine proteases (Werb, 1997; Lutolf and Hubbell, 2005). The classical synthetic polymers used in tissue engineering, such as poly-lactic acid (PLA), poly-glycolic acid (PGA) and their copolymers; poly-caprolactone (PCL, Figure 1.2.), or poly(propylenefumarate) (PPF), are typical examples of synthetic scaffolds which present hydrolytic degradation (Kim *et al*., 2003; Kweon *et al*., 2003; Jonnalagadda and Robinson, 2004; Hedberg *et al*., 2005) (Figure 3.2.). These polymers can be synthesized and tuned varying the molecular weight and glycolic acid:lactic acid ratio to assess the desired degradation rate, however, the degradation products of these scaffolds are acidic. Therefore, an acidic local microenvironment may

be formed around the area of degradation which may cause damage to the surrounding cells.

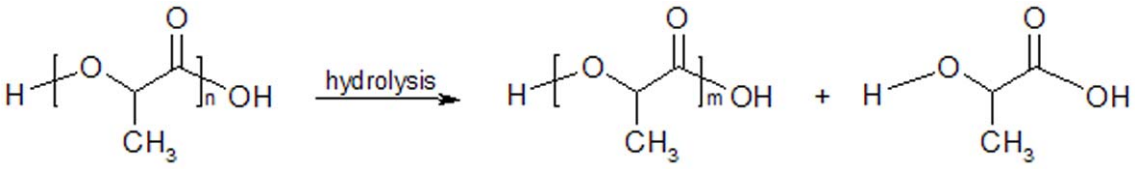

Figura 3.2. PLA hydrolysis.

Currently, special effort and progress is being made towards the synthesis of enzyme-sensitive biomaterials, containing recognition sites for proteases including matrix metalloproteinases (MMP) and serine proteases such as plasmin, elastase, or trypsin; which could be used for tissue engineering as well as for drug delivery applications. For example, Guan and Wagner (Guan and Wagner, 2005) synthesized and characterized a PCL-PEG-PCL triblock polymer coupled with the tripeptide AAK designed to present elastase sensitivity which combined both mechanism of degradation, hydrolysis and proteolysis. Pratt and co-workers (Pratt *et al*., 2004), designed PEG-bis-vinylsulfone coupled with recognition sites for plasmin. West and Hubbell (West and Hubbell, 1999) have developed PEG ABA triblock copolymers, in which the B block includes peptide sequences specific for collagenase and plasmin. In another case, Tsitlanadze *et al.* (Tsitlanadze *et al*., 2004) reported the digestion of amino-acid based poly(ester amide) scaffolds by trypsin, lipase and α-chymotrypsin. Kim and Healy (Kim and Healy, 2003) cross-linked an oligopeptide substrate for MMP-13 with Poly-(N-isopropylacrylamide-co-acrylic acid) hydrogels. In another study Lutolf and coworkers designed PEG hydrogels with both cell-adhesive properties (RGD-containing peptide) and MMP sensitive sites (Lutolf *et al*., 2003).

In this part of the work, the enzymatic degradation assays were performed on RAD16-I in order to demonstrate that these self-assembling amphiphilic peptides were protease-sensitive. The research was focused in the tryptic degradation of RAD16-I because the peptide sequence of RAD16-I has four potential cleavage sites for trypsin, as this widely studied serine-protease is known to cleave at the C-terminal of R and K, (except when the following aminoacid is a P). Firstly, thermal stability of the self-assembling peptide scaffold was studied. Circular dichroism spectra were recorded to detect secondary structure changes in the peptide scaffold when subjected to thermal denaturation. Important changes from β-sheet to random coil were observed in diluted

samples of the peptide. Then, matrix-assisted laser desorption ionization (MALDI-TOF) was used to detect the proteolytic-breakdown products of samples subjected to an incubation with trypsin, and atomic force microscopy (AFM) to visualize the effect of the degradation on the scaffold nanofibers. Samples that underwent thermal denaturation were shown to have a higher extent of degradation than non-denatured samples, as observed by AFM, suggesting that the transition from β-sheet to random coil leaves the cleavage sites accessible and susceptible to protease degradation.

3.2. RESULTS

Previous circular dichroism studies of self-assembling peptide RAD16-I showed a typical β-sheet secondary structure, presenting a minimum absorption at 218 nm and a maximum around 195 nm (Havel, 1996; Genove *et al*., 2005). This secondary structure is the basis for the self-assembly of the peptide molecules into a hydrogel formed by a network of interweaving nanofibers, and thus the applicability of the material as a scaffold in biomedical applications (Lutolf and Hubbell, 2005). Similarly, in this Thesis it is demonstrated that RAD16-I diluted in water at concentrations of 25, 50 and 75 μM, adopts a typical β-sheet structure when the spectra is recorded at room temperature (Figure 3.3., A-C). However, the peptide suffers a structural transition from β-sheet to random coil when heated at 90ºC (Figure 3.3., A-C). This change of structure is demonstrated by an abrupt shift in the maximun at 195-200 nm for a β-sheet structure to a minimum in this wavelength for the random coil configuration. This shift was shown to be irreversible at room temperature for at least a week. Surprisingly, the thermal denaturalization was not observed when concentrated solutions of peptide (5 mg/ml in water, 2.9 mM) were incubated at different temperatures, indicated by the maintenance of the β-sheet spectra in the sample incubated both at 20 ºC as well as 90 ºC (Figure 3.3., D). This is explained due to a termal stability at high peptide concentrations but not at diluted ones (2.9 mM vs 0.25 mM, respectively), indicating a concentration-dependent resistance to thermal denaturation.

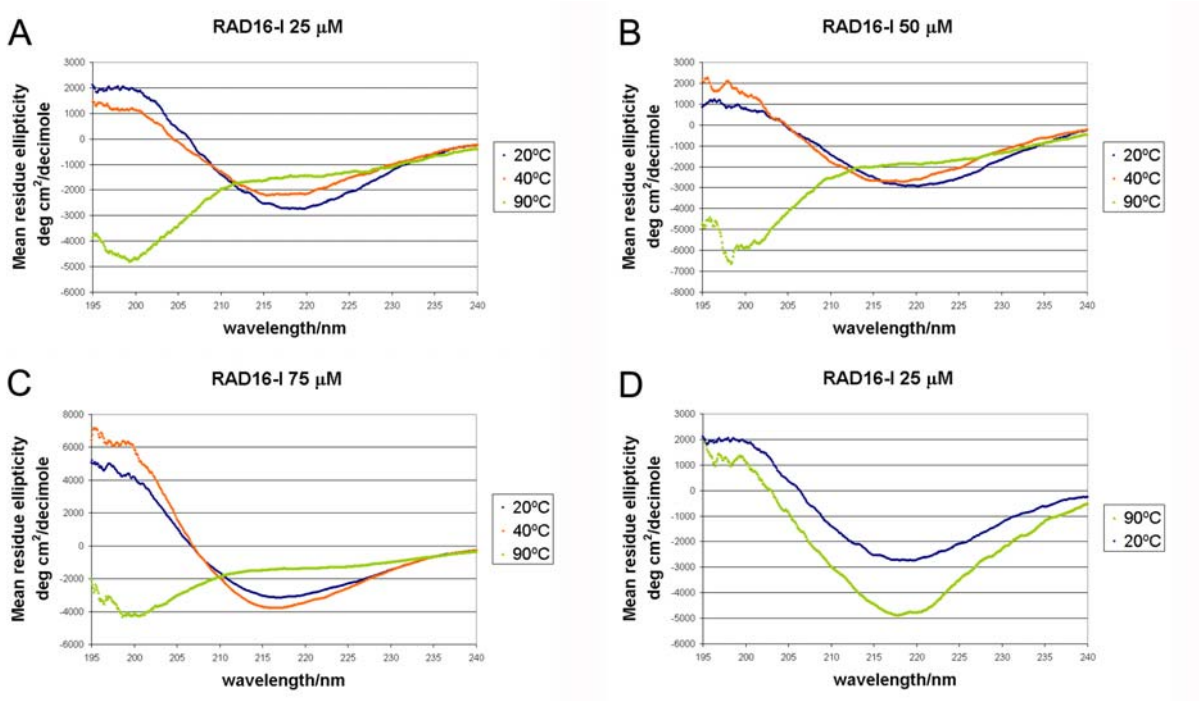

Figure 3.3. CD studies performed on peptide samples diluted in deionized water at the concentration of A) 25 μM, B) 50 μM and C) 75 μM. Spectra were recorded at different temperatures, 20, 40 and 90 ºC. D) CD studies performed on peptide samples at a final concentration of 25 μM. In this case, stock peptide samples (concentration 5 mg/ml in water, 2900 μM) were incubated at 20 ºC or 90 ºC for 10 minutes before diluting the sample to record the spectra.

AFM imaging was performed to observe the presence of nanofibers in both untreated and thermally-treated samples. Figure 3.4. A, B shows AFM images of RAD16-I at different magnifications. As it is shown, a dense network of long nanofibers is observed when a diluted solution is prepared (A and C, scale bar: 600 nm, B and D, scale bar: 250 nm). On the other hand, imaging thermally treated samples (Figure 3.4., C and D) demonstrate the presence of less amount of fibers and also the presence of shorter fibers or small pieces (Figure 3.4., D arrowheads) which indicates the loss of self-assembling capacity. This loss in the folding of the peptide may be driven by the change in the peptide secondary structure from β-sheet to random coil, as demonstrated with the CD studies (Figure 3.3.).

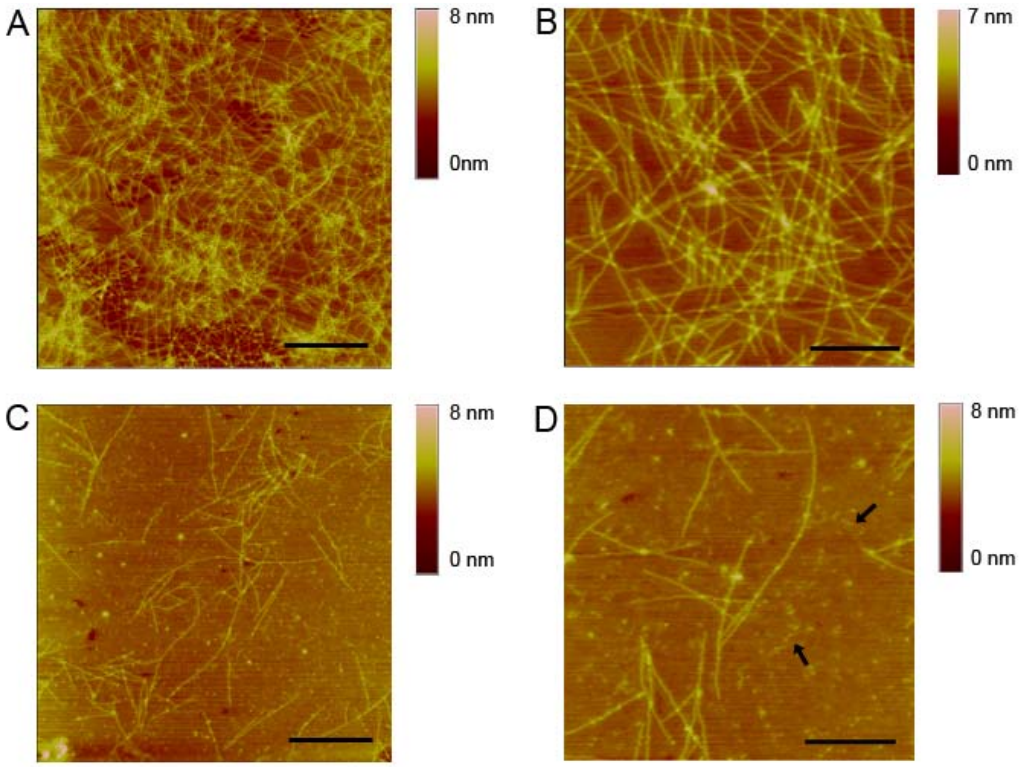

Figure 3.4. AFM images of the self-assembling peptide RAD16-I A and C) at room temperature, B and D) after a 10 min denaturation at 90 ºC. Arrowheads show small nanofiber fragments. Scale bar: A and C 600 nm, B and D 250 nm.

Furthermore, protease susceptibility of RAD16-I peptide was studied. Trypsin was chosen to perform the experiments, it is a serine protease which is known to cleave at the C-terminal of R and K (except when the following aminoacid is a proline). Trypsin is a very common enzyme widely used in molecular biology, specially, and because of its specificity, it is used in proteomic studies to perform protein identification. Thus, by observing the aminoacid sequence of the peptide (Figure 3.5.) the following peptide fragments were expected to be found (Table 3.1).

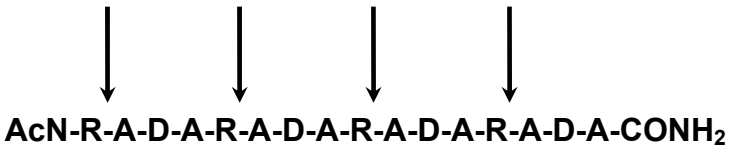

Figure 3.5. Potential cleavage sites of trypsin on RAD16-I.

Table 3.1. Theoretical peptide fragments obtained after digestion of the oligopeptide RAD16-I with trypsin.

Peptide Fragment	Molecular Weight
RAD16-I (non digested peptide)	1712
AcN-R	216
AcN-RADAR	629
AcN-RADARADAR	1043
AcN-RADARADARADAR	1456
ADA-$CONH_2$	274
ADAR	431.4
ADARADARADARADA-$CONH_2$	1514
ADARADARADA-$CONH_2$	1102
ADARADA-$CONH_2$	688
ADARADARADAR	1258
ADARADAR	844

In this sense, MALDI-TOF was used in order to evaluate RAD16-I tryptic degradation. Samples were mixed with the matrix and MALDI-TOF spectra were acquired as explained in Materials and Methods (Chapter 7). First, a RAD16-I MALDI-TOF spectra was analyzed (Figure 3.6.). It can be observed that there is mainly one peak, corresponding to RAD16-I. The indicated peaks with m/z 1642 and 1558 correspond to the peptide chain without one aminoacid residue, an alanine and an arginine respectively. These peptides most likely are impurities from the RAD16-I peptide synthesis. Moreover, different hydrolytic samples were prepared, performing or not a denaturation step at 90ºC in order to evaluate if the structural changes observed by CD had any influence on proteolytic degradation. The peptide stock solution was diluted at a concentration of 50 μM and denatured for 10 minutes at 90 ºC (with controls without temperature treatment). Then, trypsin was added to the samples in a molar ratio of 1:1000 (trypsin:peptide) followed by an incubation at 37 ºC at different periods of times indicated in each case (Figure 3.7. and Figure 3.8.). The proteolytic reaction was inactivated by boiling the samples, and finally were mixed with the matrix to acquire MALDI-TOF spectra.

Indeed, most of the expected fragments were observed in both untreated and denatured samples which are labeled on the spectra (Figure 3.7. and Figure 3.8.),

confirming the self-assembling peptide susceptibility to proteolytic degradation. The RAD16-I peak was remarkably reduced when trypsin was added to the samples. However, no apparent change was observed with time. For example, Figure 3.7. shows the spectra for A) samples after 1 minute and B) after 30 minutes of incubation with trypsin untreated samples. It can be observed that the relative intensity peak profile is practically the same in both cases. The same happens for the thermally denatured samples (Figure 3.8.). Furthermore, no differences between thermally treated and untreated samples seemed to appear (Figure 3.7. and Figure 3.8.), suggesting that the reaction have a very fast degradation kinetics regardless of the structural properties of the material used (see Discussion). Evolution of the peaks with time was plotted normalizing the peak intensity to the total intensity of the analyed peaks, in order to have comparative results from one spectra to another (Figure 3.9.). As it can be observed no evolution was observed in any of the peaks studied, which was a semi-quantitative manner to confirm what was observed with the spectra.

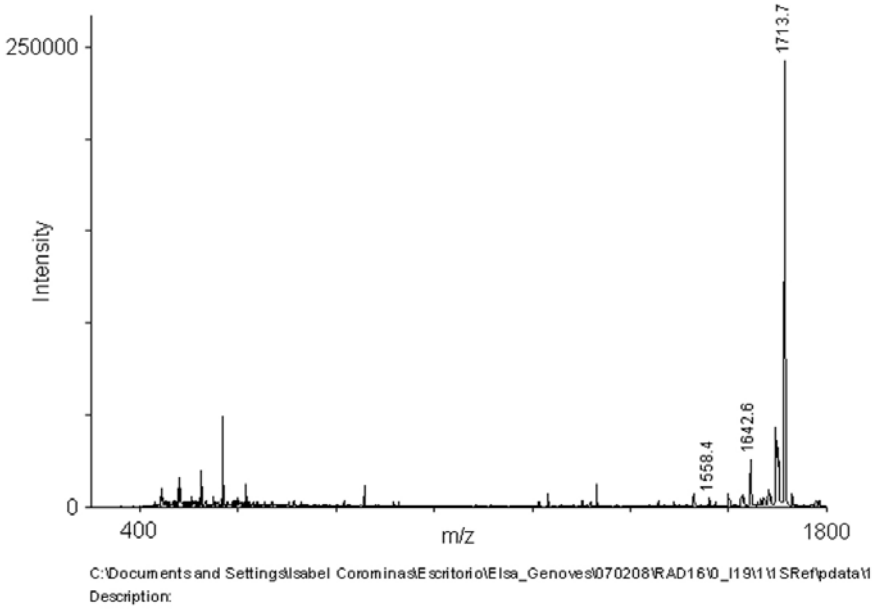

Figure 3.6. MALDI-TOF spectra of RAD16-I.

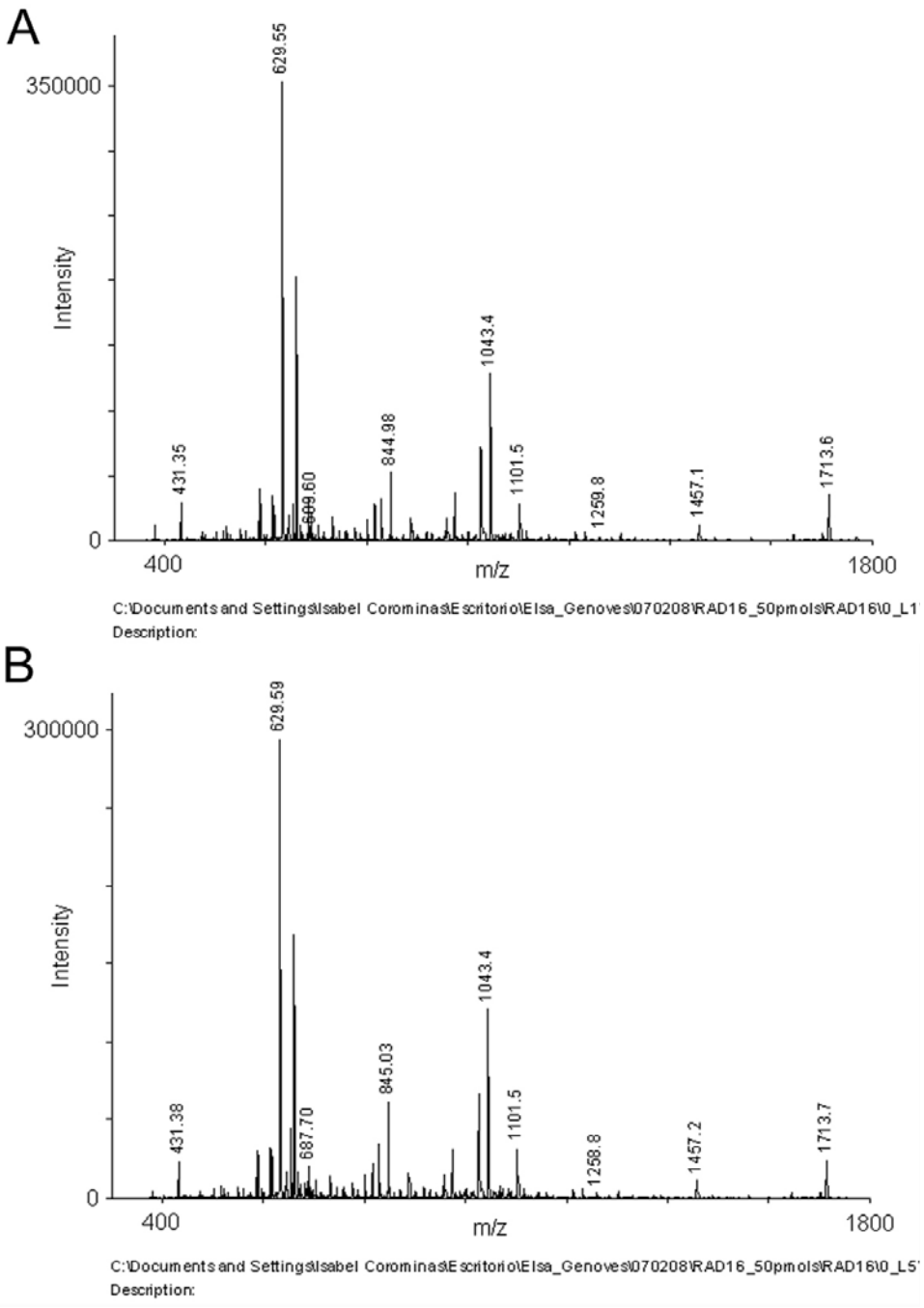

Figure 3.7. MALDI-TOF spectra RAD16-I tryptic digestion. A) After 1 minute incubation. B) After a 30 minute incubation.

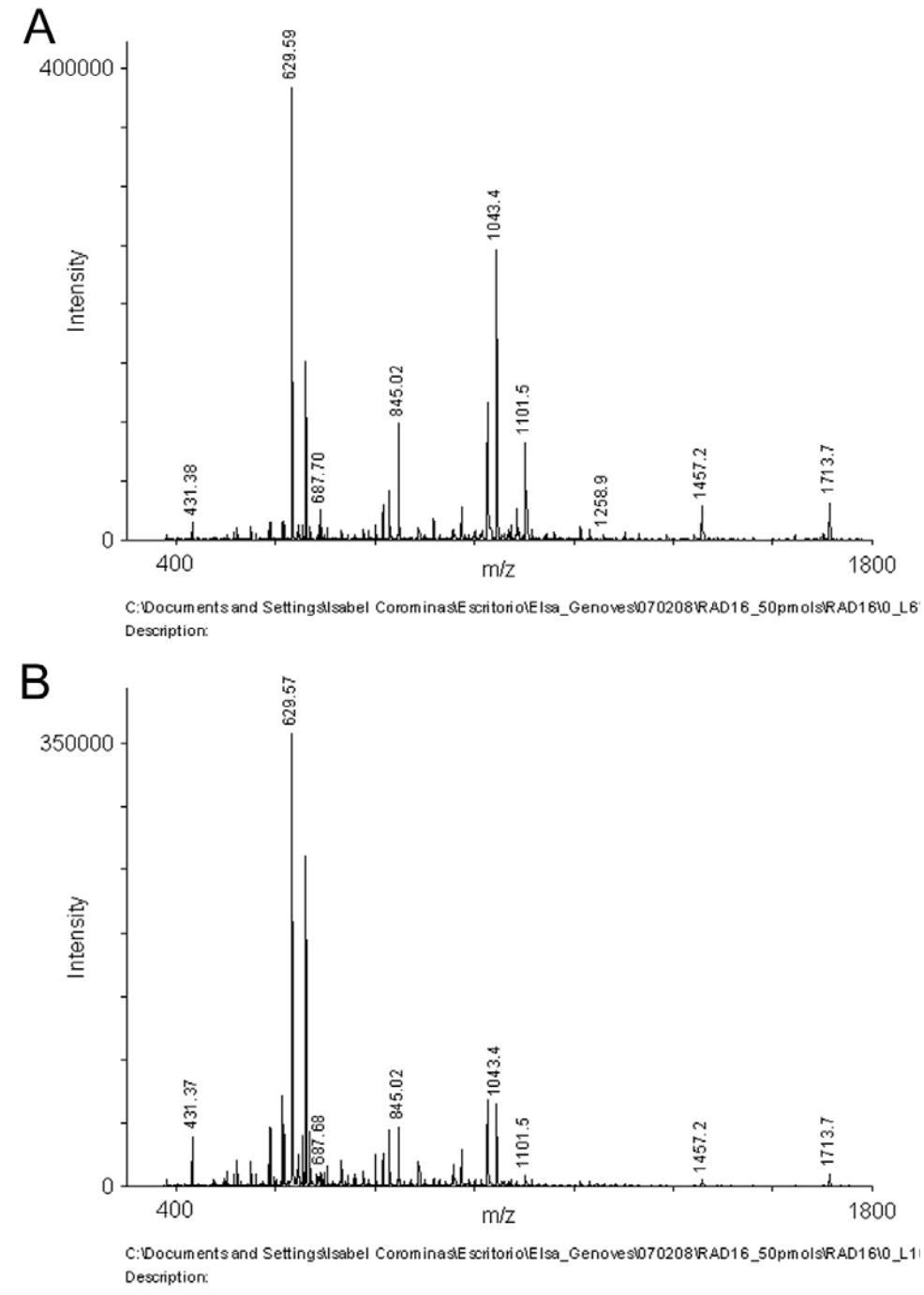

Figure 3.8. MALDI-TOF spectra of thermally denatured RAD16-I tryptic digestion. A) After 1 minute incubation. B) After a 30 minute incubation.

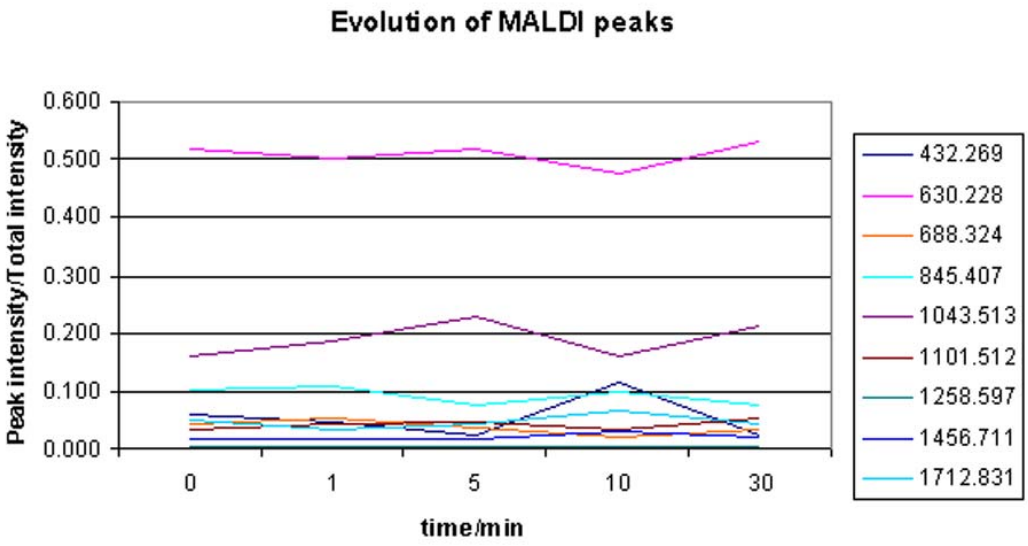

Figure 3.9. Evolution of the RAD16-I degradation peaks observed by MALDI-TOF with time.

After the results observed in the MALDI-TOF spectra, AFM images of the tryptic degradation experiments were taken. Structural changes were expected to be seen using these technique, as MALDI-TOF spectra indicated proteolysis. The same sample preparation protocol was followed to digest the samples, but ommiting the stop of the reaction (sample boiling). Samples were taken at different times and were directly spotted into freshly cleaved mica. Then, the mica was rinsed with deionized water, dried and observed under the AFM as explained in the Materials and Methods chapter (Chapter 7). Surprisingly there were strong differences between thermally treated samples and untreated samples (Figure 3.10.). It was found that, when samples were not subjected to thermal denaturation, a slight change in the nanofiber density from 10 minute to 60 minute degradation incubations was observed (Figure 3.10., A-D). However, when the samples subjected to a thermal treatment were imaged (Figure 3.10., E-H), short fibers were observed. Specially, the most typical figure seen was the cross-ramification corners, which may be less accesible to the protease. However, at long incubation times, 60 min, most of the fibers have disappeared. This disagreement between the results obtained with both techniques (MALDI-TOF and AFM), may be probably due an inefficient inactivation of trypsin when MALDI-TOF samples were prepared, in which trypsin was inactivated boiling the samples. On the contrary, when samples are spotted on freshly cleaved mica, the peptide fibers (proteins in general)

are immobilized on the surface of the mica and trypsin cannot longer perform its function.

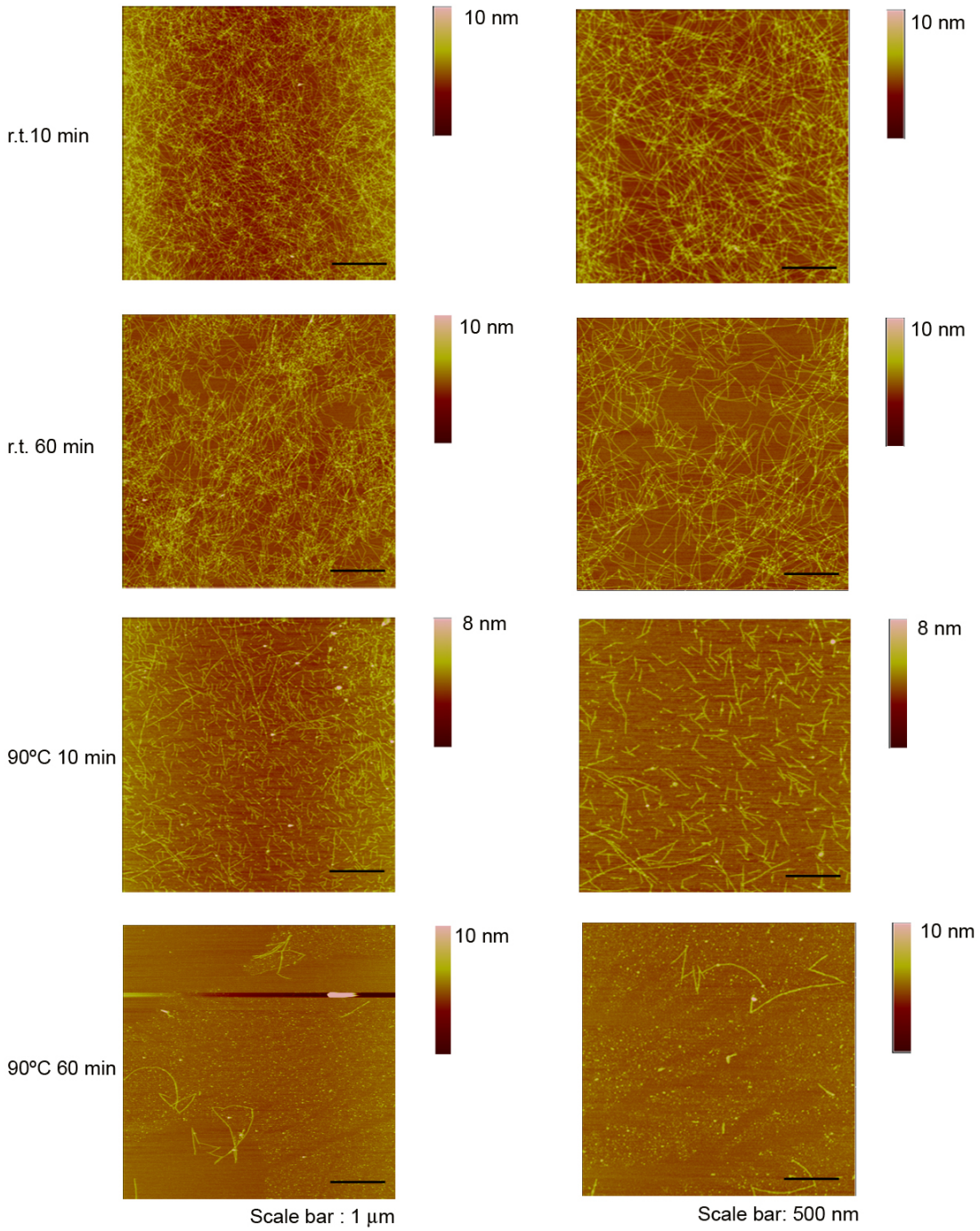

Figure 3.10. AFM images of RAD16-I tryptic degradation after different periods of time. Images indicated with r.t. correspond to samples incubated directly with trypsin, without performing a denaturation step. Images indicated with 90 ºC correspond to samples subjected to a denaturation step.

In order to solve the trypsin inactivation problems, the digestion was performed again, and the samples taken were inmediately mixed with the MALDI-TOF matrix and evaporated on the sample holder. Finally, MALDI-TOF spectra were recorded. It can be observed, that the degradation of the peptide is very fast in both cases, but there are differences in the m/z 1713 peak in the initial minutes (Figure 3.11.) suggesting an influence in peptide secondary structure in proteolytic degradation.

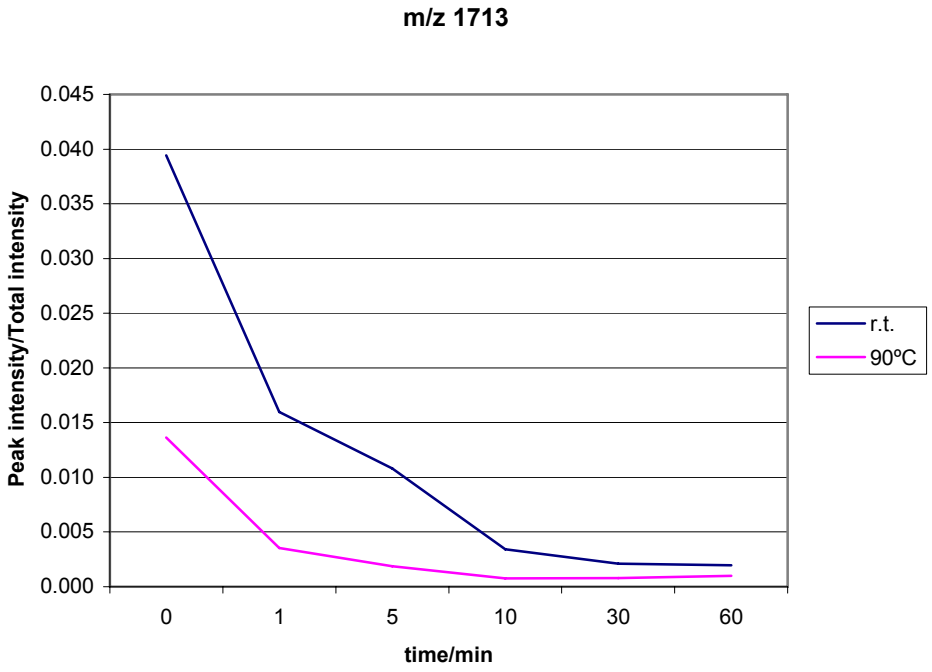

Figure 3.11. Evolution of the RAD16-I peak (m/z 1713) by MALDI-TOF in thermally treated and untreated digested samples inactivated by the MALDI-TOF sample preparation process.

3.3. DISCUSSION

In this part of the Thesis, some physicochemical and biological features of synthetic self-assembling peptide RAD16-I have been studied. This peptide is currently comercialized under the name of Puramatrix and it is being used as a scaffold in many biomedical applications and studies. Thus, in addition of performing all the necessary experiments to characterize the biological systems obtained for each different

application, it is essential to control and study all the properties regarding biodegradability of the scaffold, which up to date has not been assessed.

In the studies performed here, it has been shown that diluted solutions undergo a thermal denaturation when treated at high temperatures (Laurson *et al*., 2005) by a change of secondary structure analyzed by CD (Figure 3.3.), and confirmed by AFM.

Moreover trypsin proteolytic activity on RAD16-I was evaluated monitoring the degradation reaction with two techniques MALDI-TOF and AFM. Both techniques show a disagreement in the results, as there were no significant differences between untreated and denatured samples in spectra peaks profile and peak evolution with time. In contrast, images of different reaction time points with both samples, show remarkable differences between both samples. As stated above, this could be due an inefficient inactivation of trypsin. To achieve a total inactivation, a method other than thermal inactivation should have been used, as adding a trypsin inhibitor, lowering the pH, etc… In this manner, differences would may probably have been appreciated. In order to solve that problem, the experiment was repeated, but in this case samples taken at different times were immediately mixed with the MALDI matrix. In this way, differences were observed in the first minutes of the reaction (Figure 3.11.). The impressive differences shown by AFM added to the results obtained by circular dichroism and MALDI-TOF (Figure 3.4., Figure 3.10. and Figure 3.3.), may indicate that the change in secondary structure from β-sheet from random coil influences the proteolytic process. Indeed, the loss of the β-sheet, may leave the cleavage sites accessible for the enzymatic attack. In addition, the degradation process on untreated samples may be due to an equilibrium β-sheet-random coil in the ends of the fibers (Figure 3.12.), which also would allow trypsin accessibility to the cleavage sites.

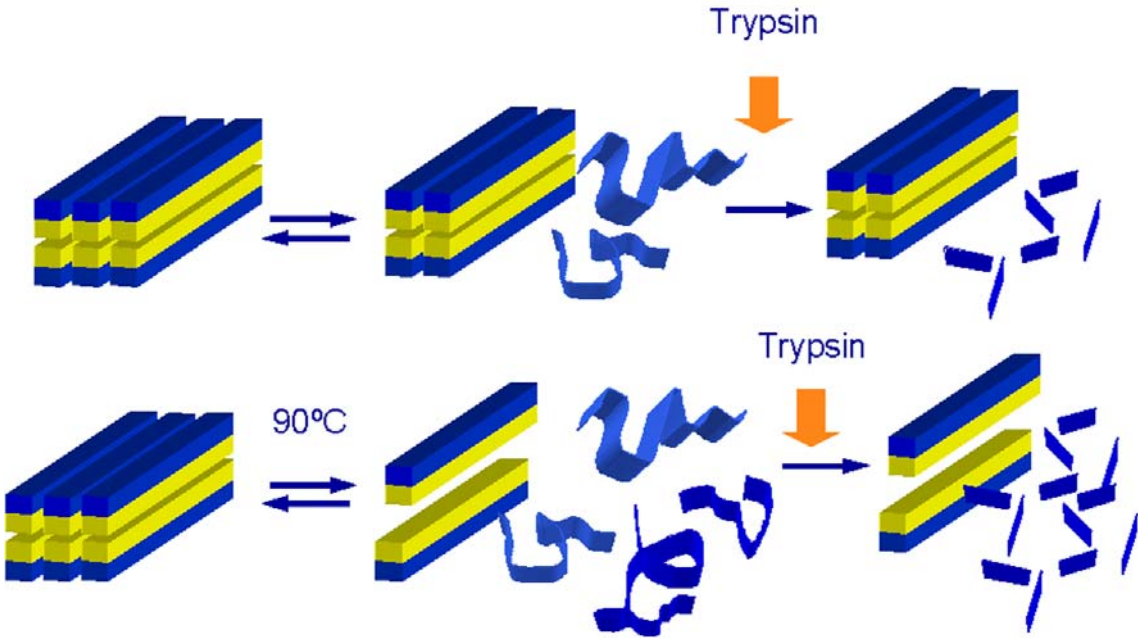

Figure 3.12. Schematic representation of the tryptic process of untreated and themally treated samples. This figure suggest that regardless of the termal treatment, trypsin peptide degradation might follow a mechanims in which terminally located peptides are in equilibrium between β-sheet and random coil. The termal treatment therefore accelerates these structural transition. In this way, the random coil peptide molecules are dissociated from the fiber endings becoming susceptible to enzyme cleavage. On the contrary, peptides located in the stable fiber structure are inaccessible to the enzyme.

As stated above, further experiments are needed to confirm this theory. The solution to the problem associated with trypsin inactivation could be solved by adding a trypsin inhibitor to stop the reaction more efficiently. However, the results obtained are a clear demonstration that the peptide is susceptible to proteolytic degradation, and open the door for future research projects involving different enzymes, such as elastase or matrix metalloproteases to further investigate the proteolytic susceptibility of these self-assembling peptide.

Moreover, these results may help in the development of more uses of RAD16-I in the biomedical field, as its proteolytic degradation has been the subject of many questions by researchers working in the field.